Disequilibrium melting of a two phase multicomponent mantle

John F. Rudge,[1,2,*] David Bercovici[1] and Marc Spiegelman[3]

[1]*Department of Geology and Geophysics, Yale University, New Haven, CT 06511, USA. E-mail: rudge@esc.cam.ac.uk*
[2]*Institute of Theoretical Geophysics, Bullard Laboratories, University of Cambridge, Madingley Road, Cambridge, CB3 0EZ, UK*
[3]*Lamont-Doherty Earth Observatory, Columbia University, Palisades, NY 10964, USA*

SUMMARY

Melt generation and segregation in Earth's mantle is typically modelled using the mixture theory of two phase flows, which combine a set of conservation laws for mass, momentum and energy with phenomenological laws for fluxes of mass and heat. Most current two phase flow models assume local thermodynamic equilibrium between melt and matrix, but geochemical observations suggest disequilibrium transport may play an important role. Here we generalise the existing two phase flow theories to encompass multiple thermodynamic components and disequilibrium. Our main focus is on the phenomenological laws describing phase change and we present general disequilibrium melting laws, which reduce to the familiar fractional and equilibrium melting laws in appropriate limits. To demonstrate the behaviour of our melting laws, we address two simple model problems for a binary system: melting at constant pressure and melting in a 1-D upwelling column at steady state. The framework presented here will prove useful in future for modelling reaction infiltration instabilities in a thermodynamically consistent manner. This framework will be useful not only for magma dynamics but for a wide range of reactive two phase flow problems.

Key words: Mid-ocean ridge processes; Mechanics, theory, and modelling; Magma genesis and partial melting; Magma migration and fragmentation.

1 INTRODUCTION

Beneath the Earth's mid-ocean ridges the mantle melts and that melt rises to the surface to form new crust. Why the mantle melts is well understood: it is a natural consequence of the thermodynamics of decompression melting (e.g. Stolper & Asimow 2007). But how the melt rises is still poorly understood, despite many decades of work on the problem. Part of the reason for this poor understanding is the complex coupling that exists between melt segregation and melt generation. To have a full description of the system we must consider not only the fluid dynamics of melt segregation but also the thermodynamics and perhaps even kinetics, of melt generation.

The main geodynamical modelling approach for this magma dynamics problem has been to use the mixture theory of two phase flows (Drew 1983). A particularly useful and highly simplified two phase flow theory appropriate to magma dynamics was written down by McKenzie (1984) and others (Scott & Stevenson 1984; Fowler 1985) and has since been applied to a wide variety of problems. In these models, melt percolates through the matrix according to Darcy's law and the matrix resists compaction through an effective bulk viscosity. More recently, these two phase flow theories have been generalised to account for additional phenomena such as sur-

face tension and damage (Bercovici *et al.* 2001; Ricard *et al.* 2001; Bercovici & Ricard 2003) and have been made more rigorous by the formal homogenisation of microscale models (Simpson *et al.* 2010a,b).

The present work seeks to extend the current two phase flow models of magma dynamics in two ways: (1) to allow chemical disequilibrium between the two phases and (2) to encompass multiple thermodynamic components. In most two phase flow models, local thermodynamic equilibrium is assumed to hold everywhere. This is a very useful assumption, as it means that the thermodynamic variables are constrained to lie on phase diagrams, which has been much exploited in recent geodynamic models (Katz 2008; Tirone *et al.* 2009). However, there is compelling geochemical evidence which suggests that melts are not always in chemical equilibrium with the matrix through which they pass (Kelemen *et al.* 1997) and indeed mantle melting is thought to be closer to a fractional process than an equilibrium process. Chemical disequilibrium has been invoked in models of the reaction infiltration instability (Aharonov *et al.* 1995; Spiegelman *et al.* 2001), a mechanism that may explain the focusing of melt into channels, promoting rapid transport of the melt.

Recent models of reactive transport have used somewhat ad hoc linear kinetic laws to describe mass transfer between phases, but the aim here is to provide a more rigorous treatment. For single component melting, two phase flow equations encompassing chemical

*Now at: Institute of Theoretical Geophysics, Bullard Laboratories, UK.

disequilibrium were derived by Sramek *et al.* (2007) (although no disequilibrium calculations were performed). Sramek *et al.* (2007) invoked the theory of non-equilibrium thermodynamics (e.g. de Groot & Mazur 1984) to provide linear phenomenological laws for disequilibrium melting and we follow their approach in our generalisation to multiple components.

The manuscript is organised as follows: First, we write down the equations governing conservation of mass, momentum and energy. The set of governing equations are completed by equations of state and phenomenological laws for transfer of heat and mass between and within the phases. The main focus here is on the phenomenological laws governing transfer of mass between the phases (i.e. melting, crystallisation, or dissolution). Non-equilibrium thermodynamics provides a theoretical basis for linear phenomenological laws, but it seems that non-linear laws are required if fractional melting is to be described accurately. Finally, the theory is applied to two well-studied model problems for a binary system: melting due to increasing temperature at constant pressure and melting by decompression in a upwelling 1-D column.

2 MASS

In what follows, subscripts refer to the individual phases (either the fluid melt *f* or solid matrix *s*) and superscripts to the components $(1, 2, \ldots, n)$.

2.1 Phases

Conservation of mass for the two phases is

$$\frac{\partial \left(\phi \rho_f\right)}{\partial t} + \nabla \cdot \left(\phi \rho_f \mathbf{v}_f\right) = \Gamma, \tag{1}$$

$$\frac{\partial \left((1-\phi)\rho_s\right)}{\partial t} + \nabla \cdot \left((1-\phi)\rho_s \mathbf{v}_s\right) = -\Gamma, \tag{2}$$

where ϕ is the porosity (the volume fraction of melt), ρ_f and ρ_s are densities and $\mathbf{v}_f$ and $\mathbf{v}_s$ are velocities of the fluid and solid respectively. Γ represents the total rate of mass exchange from solid phase to fluid phase (the melting rate). It follows that given any scalar quantities a_f and a_s per unit mass we have

$$\frac{\partial \left(\phi \rho_f a_f\right)}{\partial t} + \nabla \cdot \left(\phi \rho_f a_f \mathbf{v}_f\right) = \phi \rho_f \frac{D_f a_f}{Dt} + \Gamma a_f, \tag{3}$$

$$\frac{\partial \left((1-\phi)\rho_s a_s\right)}{\partial t} + \nabla \cdot \left((1-\phi)\rho_s a_s \mathbf{v}_s\right) = (1-\phi)\,\rho_s \frac{D_s a_s}{Dt} - \Gamma a_s, \tag{4}$$

where D_f/Dt and D_s/Dt are Lagrangian derivatives following the fluid and solid, respectively. It follows that

$$\frac{\partial}{\partial t} \left(\phi \rho_f a_f + (1-\phi)\rho_s a_s\right) + \nabla \cdot \left(\phi \rho_f a_f \mathbf{v}_f + (1-\phi)\rho_s a_s \mathbf{v}_s\right)$$
$$= \phi \rho_f \frac{D_f a_f}{Dt} + (1-\phi)\,\rho_s \frac{D_s a_s}{Dt} - \Gamma \Delta a, \tag{5}$$

where $\Delta a = a_s - a_f$. These expressions are useful in writing the conservation equations to come in a more compact form, as throughout expressions will be cast in terms of Lagrangian derivatives.

The mass conservation eqs (1) and (2) can be rewritten in Lagrangian form as

$$\nabla \cdot \mathbf{v}_f = -\frac{1}{\phi}\frac{D_f \phi}{Dt} + \rho_f \frac{D_f(1/\rho_f)}{Dt} + \frac{\Gamma}{\phi \rho_f}, \tag{6}$$

$$\nabla \cdot \mathbf{v}_s = \frac{1}{1-\phi}\frac{D_s \phi}{Dt} + \rho_s \frac{D_s(1/\rho_s)}{Dt} - \frac{\Gamma}{(1-\phi)\rho_s}. \tag{7}$$

Similarly, the mean velocity $\bar{\mathbf{v}} \equiv \phi \mathbf{v}_f + (1-\phi)\mathbf{v}_s = \phi(\mathbf{v}_f - \mathbf{v}_s) + \mathbf{v}_s$ satisfies

$$\nabla \cdot \bar{\mathbf{v}} = \phi \rho_f \frac{D_f(1/\rho_f)}{Dt} + (1-\phi)\rho_s \frac{D_s(1/\rho_s)}{Dt} - \Gamma \Delta(1/\rho), \tag{8}$$

where $\Delta(1/\rho) = 1/\rho_s - 1/\rho_f$. It is often more convenient to work with mass conservation in the form of (7) and (8) rather than (1) and (2).

2.2 Components

The two phases are made up of *n* thermodynamic components e.g. if the phases were pure olivine, component 1 could be Mg_2SiO_4 (forsterite) and component 2 could be Fe_2SiO_4 (fayalite). Conservation of components is

$$\phi \rho_f \frac{D_f c_f^j}{Dt} + \Gamma c_f^j = -\nabla \cdot \mathbf{J}_f^j + \Gamma^j, \tag{9}$$

$$(1-\phi)\,\rho_s \frac{D_s c_s^j}{Dt} - \Gamma c_s^j = -\nabla \cdot \mathbf{J}_s^j - \Gamma^j, \tag{10}$$

where the left hand sides of the above equations have been written in Lagrangian form using (3) and (4). c_f^j and c_s^j are the concentrations by mass of component *j* in the two phases. Γ^j represents the rate of mass exchange of component *j* from solid to fluid (interphase exchange), whereas $\mathbf{J}_f^j$ and $\mathbf{J}_s^j$ represent the diffusive mass fluxes of component *j* within the fluid and solid phases respectively (intraphase fluxes). For consistency with the conservation of mass eqs (1) and (2), the following constraints hold

$$\sum_j c_f^j = \sum_j c_s^j = 1, \tag{11}$$

$$\sum_j \mathbf{J}_f^j = \sum_j \mathbf{J}_s^j = 0, \tag{12}$$

$$\Gamma = \sum_j \Gamma^j. \tag{13}$$

The first of these constraints simply states that c_f^j and c_s^j represent the compositions of the two phases and thus must sum to 1. Eq. (12) states that the diffusive intraphase fluxes must sum to zero and (13) states that the total rate of interphase mass transfer from solid to liquid is given by the sum of the mass exchanges from solid to liquid of the individual components.

3 MOMENTUM

Derivations of the equations governing conservation of momentum are much more involved than those governing conservation of mass and have been discussed in detail by many other authors (McKenzie 1984; Scott & Stevenson 1984; Fowler 1985; Schmeling 2000; Bercovici *et al.* 2001; Ricard *et al.* 2001; Bercovici & Ricard 2003; Simpson *et al.* 2010a,b). Only a brief outline of their derivation is given here.

Conservation of momentum for the slow creeping flow of the two phases is

$$\nabla \cdot \left(\phi \boldsymbol{\sigma}_f\right) + \phi \rho_f \mathbf{g} = \mathbf{F}, \tag{14}$$

$$\nabla \cdot ((1 - \phi)\,\boldsymbol{\sigma}_s) + (1 - \phi)\,\rho_s \mathbf{g} = -\mathbf{F}, \tag{15}$$

where $\mathbf{F}$ is the interphase force per unit volume, representing the force one phase exerts on the other and $\mathbf{g}$ is the acceleration due to gravity. $\boldsymbol{\sigma}_f$ and $\boldsymbol{\sigma}_s$ are the stress tensors for the two phases. It is assumed that locally components within the same phase feel the same stress, but that different phases feel different stresses. Hence only two momentum equations are needed (one for each phase), rather than the $2n$ equations that are needed to describe conservation of mass (one for each phase and $2(n-1)$ for the components).

Eqs (14) and (15) can be summed to give the total conservation of momentum equation

$$\nabla \cdot \overline{\boldsymbol{\sigma}} + \overline{\rho}\mathbf{g} = \mathbf{0}, \tag{16}$$

where the average stress tensor and density are defined by

$$\overline{\boldsymbol{\sigma}} = \phi\boldsymbol{\sigma}_f + (1 - \phi)\,\boldsymbol{\sigma}_s, \tag{17}$$

$$\overline{\rho} = \phi\rho_f + (1 - \phi)\,\rho_s. \tag{18}$$

Mechanical pressures for the two phases are defined in the standard way by

$$p_f = -\frac{1}{3}\,\operatorname{tr}\boldsymbol{\sigma}_f, \tag{19}$$

$$p_s = -\frac{1}{3}\,\operatorname{tr}\boldsymbol{\sigma}_s, \tag{20}$$

with a mean mechanical pressure given by

$$\overline{p} = -\frac{1}{3}\,\operatorname{tr}\overline{\boldsymbol{\sigma}} = \phi p_f + (1 - \phi)p_s. \tag{21}$$

The stress tensors can be split into isotropic and deviatoric (trace-free) parts as

$$\boldsymbol{\sigma}_f = -p_f\mathbf{I} + \boldsymbol{\tau}_f, \tag{22}$$

$$\boldsymbol{\sigma}_s = -p_s\mathbf{I} + \boldsymbol{\tau}_s, \tag{23}$$

where $\boldsymbol{\tau}_f$ and $\boldsymbol{\tau}_s$ are the deviatoric stress tensors and $\mathbf{I}$ is the identity tensor.

A simple phenomenological law for the interphase force $\mathbf{F}$ is given by (Drew 1983)

$$\mathbf{F} = d\,(\mathbf{v}_f - \mathbf{v}_s) - P\nabla\phi, \tag{24}$$

where d is a drag coefficient associated with resistance of motion of the two phases past each other and P is the interface pressure, which produces a net force if porosity spatially varies. Throughout this work we will neglect surface tension, but a generalisation of the above law to encompass surface tension effects can be found in Bercovici *et al.* (2001).

To complete the set of equations, phenomenological laws are needed to determine the pressure differences $P - p_f$ and $P - p_s$ and the deviatoric stress tensors $\boldsymbol{\tau}_f$ and $\boldsymbol{\tau}_s$. To be consistent with the simplified two phase flow theory of McKenzie (1984), the phenomenological laws must take the form

$$P - p_f = 0, \tag{25}$$

$$P - p_s = \frac{\zeta_\phi}{1 - \phi}\nabla \cdot \mathbf{v}_s, \tag{26}$$

$$\boldsymbol{\tau}_f = \mathbf{0}, \tag{27}$$

$$\boldsymbol{\tau}_s = \frac{\eta_\phi}{1 - \phi}\left(\nabla\mathbf{v}_s + \nabla\mathbf{v}_s^T - \frac{2}{3}(\nabla \cdot \mathbf{v}_s)\mathbf{I}\right). \tag{28}$$

These laws appear somewhat asymmetric due to an assumption that the matrix is much more viscous that the melt. (14), (24), (25) and (27) then lead to the usual Darcy's law for the melt,

$$\phi\,(\mathbf{v}_f - \mathbf{v}_s) = -\frac{k_\phi}{\mu}\,(\nabla P - \rho_f\mathbf{g}), \tag{29}$$

where the permeability k_ϕ (a function of porosity) is related to the drag coefficient by $d = \mu\phi^2/k_\phi$. (16) and (25)–(28) lead to a total conservation of momentum equation

$$\nabla P = \nabla \cdot \left(\eta_\phi\,(\nabla\mathbf{v}_s + \nabla\mathbf{v}_s^T)\right) + \nabla\left(\left(\zeta_\phi - \frac{2}{3}\eta_\phi\right)\nabla \cdot \mathbf{v}_s\right) + \overline{\rho}\mathbf{g}, \tag{30}$$

which resembles the equation governing compressible Stokes flow, where η_ϕ and ζ_ϕ can be interpreted as effective shear and bulk viscosities for the two phase mixture (which are also porosity dependent). More general phenomenological laws than those in (25)–(28) were developed by Bercovici & Ricard (2003) to preserve material invariance and these laws are outlined briefly in Appendix A (also see discussion in Simpson *et al.* 2010a).

4 ENERGY

When considering the thermodynamics of two phase flow, as we must when considering conservation of energy, a key difficulty is the notion of pressure and in particular the difference between 'thermodynamic' and 'mechanical' definitions of pressure. The thermodynamic pressure appears in definitions of thermodynamic potentials for example, in the relationship between enthalpy and internal energy, $H = U + pV$. The mechanical pressures are defined by minus one third the trace of the stress tensor, as in (19), (20) and (21). Even for a compressible single phase viscous fluid there is difference between these two definitions of pressure. This difference depends on the bulk viscosity and the divergence of the velocity field and disappears in equilibrium. For a two phase system, the situation is much less clear as there are multiple mechanical pressures and potentially multiple thermodynamic pressures.

In what follows all thermodynamic potentials for both phases are defined with P, the interface pressure, as the appropriate thermodynamic pressure. There is some justification for this in the work of Sramek *et al.* (2007) where it was shown that this leads to a particularly natural characterisation of phase change. For the phenomenological laws considered, the difference between mechanical and thermodynamic pressures only depends on the divergences of the velocity fields, in a way analogous to the compressible single phase case. Using P for the thermodynamic pressure is also identical to the assumption made by McKenzie (1984) where the fluid pressure (identical to the interface pressure, 25) was chosen as the common thermodynamic pressure for the two phases. Nevertheless, thermodynamic pressure remains a thorny aspect of two phase flow theories and deserves further careful study.

Conservation of total internal energy is (McKenzie 1984; de Groot & Mazur 1984)

$$\begin{aligned}
\phi\rho_f\frac{\mathrm{D}_f u_f}{\mathrm{D}t} &+ (1 - \phi)\,\rho_s\frac{\mathrm{D}_s u_s}{\mathrm{D}t} - \Gamma\Delta u \\
&= Q - \nabla \cdot \mathbf{q} + \nabla \cdot \left(\phi\boldsymbol{\sigma}_f \cdot \mathbf{v}_f + (1 - \phi)\,\boldsymbol{\sigma}_s \cdot \mathbf{v}_s\right) + \phi\rho_f\mathbf{v}_f \cdot \mathbf{g} \\
&\quad + (1 - \phi)\,\rho_s\mathbf{v}_s \cdot \mathbf{g},
\end{aligned} \tag{31}$$

where u_f and u_s are the internal energies per unit mass of the two phases, Q is the rate of internal heat production (e.g. from radioactivity), $\mathbf{q}$ is the diffusive heat flux and the remaining terms

on the right hand side are sources of energy due to work. Using the momentum eqs ((14), (15) and (24)), the energy equation can be simplified to

$$\phi \rho_f \frac{D_f u_f}{Dt} + (1 - \phi) \rho_s \frac{D_s u_s}{Dt} - \Gamma \Delta u = Q - \nabla \cdot \mathbf{q} - P \nabla \cdot \bar{\mathbf{v}} + \Psi, \tag{32}$$

where Ψ is the viscous dissipation,

$$\Psi = d (\mathbf{v}_f - \mathbf{v}_s)^2 + \phi (P - p_f) \nabla \cdot \mathbf{v}_f + (1 - \phi)(P - p_s) \nabla \cdot \mathbf{v}_s$$
$$+ \phi \boldsymbol{\tau}_f : \nabla \mathbf{v}_f + (1 - \phi) \boldsymbol{\tau}_s : \nabla \mathbf{v}_s. \tag{33}$$

With the simplified phenomenological laws (25)–(28), the viscous dissipation can be written as

$$\Psi = \frac{\mu \phi^2}{k_\phi} (\mathbf{v}_f - \mathbf{v}_s)^2 + \zeta_\phi (\nabla \cdot \mathbf{v}_s)^2$$
$$+ \frac{\eta_\phi}{2} \left(\nabla \mathbf{v}_s + \nabla \mathbf{v}_s^T - \frac{2}{3} \mathbf{I} (\nabla \cdot \mathbf{v}_s) \right)^2. \tag{34}$$

Here squares represent a dot product for vectors $\mathbf{a}^2 = \mathbf{a} \cdot \mathbf{a}$ and a double dot product for second rank tensors $\mathbf{A}^2 = \mathbf{A} : \mathbf{A}$. A more general expression for the viscous dissipation can be found in Section A using the phenomenological laws of Bercovici & Ricard (2003).

Conservation of energy (32) can be rewritten using conservation of mass (8) as

$$\phi \rho_f \frac{D_f u_f}{Dt} + (1 - \phi) \rho_s \frac{D_s u_s}{Dt} - \Gamma \Delta u$$
$$= Q - \nabla \cdot \mathbf{q} - P \left(\phi \rho_f \frac{D_f (1/\rho_f)}{Dt} + (1 - \phi) \rho_s \frac{D_s (1/\rho_s)}{Dt} \right.$$
$$\left. - \Gamma \Delta (1/\rho) \right) + \Psi. \tag{35}$$

In applications it is useful to rewrite the energy equation in terms of different thermodynamic potentials. For example, specific enthalpy satisfies

$$h_i = u_i + \frac{P}{\rho_i}, \qquad \frac{D_i h_i}{Dt} = \frac{D_i u_i}{Dt} + \frac{1}{\rho_i} \frac{D_i P}{Dt} + P \frac{D_i (1/\rho_i)}{Dt}, \tag{36}$$

where the subscript i refers to the phase, $i = s, f$. As discussed above, the definition of specific enthalpy used here is in terms of the interface pressure P. Using (36), conservation of energy (31) can be written as an enthalpy equation

$$\phi \rho_f \frac{D_f h_f}{Dt} + (1 - \phi) \rho_s \frac{D_s h_s}{Dt} - \Gamma \Delta h$$
$$= \phi \frac{D_f P}{Dt} + (1 - \phi) \frac{D_s P}{Dt} + Q - \nabla \cdot \mathbf{q} + \Psi, \tag{37}$$

which is the form of the energy equation used in the enthalpy method (Katz 2008). We will return to this enthalpy equation in Section 6 to write a temperature equation.

4.1 Entropy

Perhaps the most important rewriting of the energy equation is as an equation for entropy. Since

$$h_i = T s_i + \sum_j \mu_i^j c_i^j, \qquad \frac{D_i h_i}{Dt} = T \frac{D_i s_i}{Dt} + \frac{1}{\rho_i} \frac{D_i P}{Dt} + \sum_j \mu_i^j \frac{D_i c_i^j}{Dt}, \tag{38}$$

the enthalpy equation (37) can be written as an entropy equation,

$$T \phi \rho_f \frac{D_f s_f}{Dt} + T (1 - \phi) \rho_s \frac{D_s s_s}{Dt} - \Gamma T \Delta s$$
$$= Q - \nabla \cdot \mathbf{q} + \Psi + \sum_j \left(\mu_f^j \nabla \cdot \mathbf{J}_f^j + \mu_s^j \nabla \cdot \mathbf{J}_s^j + \Gamma^j \Delta \mu^j \right), \tag{39}$$

where we have used conservation of components (9), (10). The above expression can be written as an entropy balance,

$$\phi \rho_f \frac{D_f s_f}{Dt} + (1 - \phi) \rho_s \frac{D_s s_s}{Dt} - \Gamma \Delta s = -\nabla \cdot \mathbf{j} + \sigma, \tag{40}$$

where $\mathbf{j}$ is the entropy flux and σ is the entropy production. Comparing (39) and (40), we see that the entropy flux $\mathbf{j}$ is related to fluxes of heat and components by

$$\mathbf{j} = \frac{\mathbf{q}}{T} - \sum_j \frac{\mathbf{J}_f^j \mu_f^j + \mathbf{J}_s^j \mu_s^j}{T} \tag{41}$$

and the entropy production σ is given by

$$\sigma = \frac{1}{T} \left(Q + \Psi - \mathbf{j} \cdot \nabla T + \sum_j \Gamma^j \Delta \mu^j - \mathbf{J}_f^j \cdot \nabla \mu_f^j - \mathbf{J}_s^j \cdot \nabla \mu_s^j \right). \tag{42}$$

The second law of thermodynamics requires that $\sigma \geq 0$ (also known as the Clausius–Duhem inequality).

5 EQUATIONS OF STATE

Equations of state need to be prescribed for the two phases. In theory, this could be done using the internal energy, by specifying functions $u_i(s_i, \rho_i, c_i^j)$ for the two phases. The temperature, pressure and chemical potentials could then be derived from these functions using the Gibbs relation $du_i = T ds_i - P d(1/\rho_i) + \sum_j \mu_i^j dc_i^j$ or

$$T = \frac{\partial u_i}{\partial s_i}, \quad P = -\frac{\partial u_i}{\partial (1/\rho_i)}, \quad \mu_i^j = \frac{\partial u_i}{\partial c_i^j}. \tag{43}$$

However, thermodynamic data is not usually given in (s_i, ρ_i, c_i^j) co-ordinates, but rather in (P, T, c_i^j) co-ordinates and it is helpful to re-express the equations of state. Such co-ordinates are also useful since we are assuming a common temperature T and interface pressure P for both phases. The co-ordinate change uses the following standard partial derivatives in (P, T, c_i^j) co-ordinates,

$$\alpha_i = \rho_i \frac{\partial (1/\rho_i)}{\partial T}, \qquad \beta_i = -\rho_i \frac{\partial (1/\rho_i)}{\partial P}, \tag{44}$$

$$C_i = T \frac{\partial s_i}{\partial T} = \frac{\partial h_i}{\partial T}, \tag{45}$$

α_i is the thermal expansion coefficient, β_i is the isothermal compressibility and C_i is the specific heat capacity at constant pressure. The dependence on composition is captured by introducing partial specific quantities as

$$h_i = \sum_j c_i^j h_i^j, \qquad \frac{1}{\rho_i} = \sum_j \frac{c_i^j}{\rho_i^j}, \tag{46}$$

where $1/\rho_i^j$ is the partial specific volume of component j in phase i and h_i^j is the corresponding partial specific enthalpy. Using (44)–(46), we may then write equations of state in terms of Lagrangian derivatives

$$\rho_i \frac{D_i (1/\rho_i)}{Dt} = \alpha_i \frac{D_i T}{Dt} - \beta_i \frac{D_i P}{Dt} + \sum_j \frac{\rho_i}{\rho_i^j} \frac{D_i c_i^j}{Dt}, \tag{47}$$

$$\frac{D_i h_i}{Dt} = C_i \frac{D_i T}{Dt} + \frac{1 - \alpha_i T}{\rho_i} \frac{D_i P}{Dt} + \sum_j h_i^j \frac{D_i c_i^j}{Dt}. \tag{48}$$

Of course, the quantities α_i, β_i, etc. may be functions of P, T and c_i^j but are often assumed constant for simplicity. Equations of state are also needed to describe the chemical potentials μ_i^j and these are discussed later in Section 7.

6 TEMPERATURE EQUATIONS

Using (47) we may rewrite the mass conservation eqs (6) and (7) as

$$\nabla \cdot \mathbf{v}_f = -\frac{1}{\phi} \frac{D_f \phi}{Dt} + \alpha_f \frac{D_f T}{Dt} - \beta_f \frac{D_f P}{Dt} + \sum_j \frac{\Gamma^j - \nabla \cdot \mathbf{J}_f^j}{\phi \rho_f^j}, \tag{49}$$

$$\nabla \cdot \mathbf{v}_s = \frac{1}{1 - \phi} \frac{D_s \phi}{Dt} + \alpha_s \frac{D_s T}{Dt} - \beta_s \frac{D_s P}{Dt} - \sum_j \frac{\Gamma^j + \nabla \cdot \mathbf{J}_s^j}{(1 - \phi) \rho_s^j}, \tag{50}$$

where the derivatives of composition have been removed using conservation of components (9), (10). The corresponding equation for the mean velocity (8) becomes

$$\nabla \cdot \overline{\mathbf{v}} = \phi \alpha_f \frac{D_f T}{Dt} + (1 - \phi) \alpha_s \frac{D_s T}{Dt} - \phi \beta_f \frac{D_f P}{Dt} - (1 - \phi) \beta_s \frac{D_s P}{Dt}$$
$$- \sum_j \left(\Gamma^j \Delta(1/\rho^j) + \frac{\nabla \cdot \mathbf{J}_f^j}{\rho_f^j} + \frac{\nabla \cdot \mathbf{J}_s^j}{\rho_s^j} \right).$$

Using (48), the conservation of energy eq. (37) can be rewritten as

$$\phi \rho_f C_f \frac{D_f T}{Dt} + (1 - \phi) \rho_s C_s \frac{D_s T}{Dt} - \phi \alpha_f T \frac{D_f P}{Dt}$$
$$- (1 - \phi) \alpha_s T \frac{D_s P}{Dt}$$
$$= Q + \Psi - \nabla \cdot \mathbf{q}' + \sum_j \left(\Gamma^j \Delta h^j - \mathbf{J}_f^j \cdot \nabla h_f^j - \mathbf{J}_s^j \cdot \nabla h_s^j \right), \tag{51}$$

where again the derivatives of composition have been removed using conservation of components (9), (10). $\mathbf{q}'$ is an alternative definition of heat flux, related to the original fluxes by

$$\mathbf{q}' = \mathbf{q} - \sum_j \mathbf{J}_f^j h_f^j + \mathbf{J}_s^j h_s^j. \tag{52}$$

The temperature eq. (51) can also be written in terms of averaged quantities,

$$\overline{\rho C} \frac{\partial T}{\partial t} + \overline{\rho C \mathbf{v}} \cdot \nabla T - T \overline{\alpha} \frac{\partial P}{\partial t} - T \overline{\alpha \mathbf{v}} \cdot \nabla P$$
$$= Q + \Psi - \nabla \cdot \mathbf{q}' - \sum_j \left(\Gamma^j L^j + \mathbf{J}_f^j \cdot \nabla h_f^j + \mathbf{J}_s^j \cdot \nabla h_s^j \right), \tag{53}$$

where $L^j = -\Delta h^j = h_f^j - h_s^j$ is the latent heat (enthalpy of fusion) for melting of component j and the overbars represent averages as

$$\overline{\rho C} = \phi \rho_f C_f + (1 - \phi) \rho_s C_s, \tag{54}$$

$$\overline{\rho C \mathbf{v}} = \phi \rho_f C_f \mathbf{v}_f + (1 - \phi) \rho_s C_s \mathbf{v}_s, \tag{55}$$

$$\overline{\alpha} = \phi \alpha_f + (1 - \phi) \alpha_s, \tag{56}$$

$$\overline{\alpha \mathbf{v}} = \phi \alpha_f \mathbf{v}_f + (1 - \phi) \alpha_s \mathbf{v}_s. \tag{57}$$

The temperature eq. (53) closely resembles the standard temperature equation for single phase flow. The two phase nature of the flow appears in the averaging of specific heat capacities, thermal expansivities and velocities and through the latent heat term. The multicomponent nature of the flow appears in the terms involving diffusive fluxes of components, the different latent heats for the different components and the potential for composition dependent properties.

7 CHEMICAL POTENTIALS

To have a full description of the thermodynamics, we need to relate chemical potentials to temperature, pressure and composition. It is an unfortunate fact that when working with chemical potentials we have to deal with both mass fractions (denoted by c^j) and mole fractions (denoted by x^j). It is straightforward to convert between the two sets of variables:

$$c^j = \frac{M^j x^j}{M}, \qquad x^j = \frac{M c^j}{M^j}, \tag{58}$$

where M^j are the molar masses of each component (kg mol^{-1}) and M is the mean molar mass, given by

$$M = \sum_j M^j x^j = \left(\sum_j \frac{c^j}{M^j} \right)^{-1}. \tag{59}$$

Another way of expressing these relationships is by

$$c^j = \left\{ M^j x^j \right\}, \qquad x^j = \left\{ c^j / M^j \right\}, \tag{60}$$

where $\{\cdot\}$ refers to normalising to unit sum, $\left\{ a^j \right\} = a^j / \sum_k a^k$.

The chemical potentials are related to temperature, pressure and composition by the standard relationships (Spear 1993; Anderson 2005)

$$\mu_s^j = \mu_s^{j\circ}(P, T) + R^j T \log \left(\gamma_s^j x_s^j \right)^\nu, \tag{61}$$

$$\mu_f^j = \mu_f^{j\circ}(P, T) + R^j T \log \left(\gamma_f^j x_f^j \right)^\nu, \tag{62}$$

where γ^j are activity coefficients and x^j are molar concentrations. The activity model used here $(\gamma^j x^j)^\nu$ is a non-ideal one-site substitution model suitable for minerals such as olivine: for activity models for more complex assemblages the reader is encouraged to consult the textbooks (e.g. Chapter 7 of Spear 1993). The activity coefficients $\gamma^j = 1$ for an ideal solution and ν is the number of lattice sites per formula unit (e.g. $\nu = 2$ for olivine (MgFe)$_2$SiO$_4$). R^j is the specific gas constant for component j, $R^j = \tilde{R}/M^j$, where $\tilde{R}$ is the universal gas constant ($\tilde{R} = 8.314472$ J K^{-1} mol^{-1}) and M^j is the molar mass. This is consistent with the earlier definition of the chemical potential as being per unit mass (the units of μ are J kg^{-1}). The chemical potentials per mole are given by $\tilde{\mu}_s^j = \mu_s M^j$, $\tilde{\mu}_f^j = \mu_f M^j$ (with units J mol^{-1}).

The differences in chemical potentials, $\Delta \mu^j = \mu_s^j - \mu_f^j$ satisfy

$$\Delta \mu^j = -R^j T \log K^j + R^j T \log Q^j, \tag{63}$$

where K^j are the equilibrium constants, functions only of temperature and pressure, defined by

$$-R^j T \log K^j = \mu_s^{j\circ} - \mu_f^{j\circ} \tag{64}$$

and Q^j are the activity ratios, defined by

$$Q^j = \left(\frac{\gamma_s^j x_s^j}{\gamma_f^j x_f^j} \right)^\nu. \tag{65}$$

(63) can be rewritten as

$$\frac{Q^j}{K^j} = \exp\left(\frac{\Delta\mu^j}{R^j T}\right). \tag{66}$$

In equilibrium $\Delta\mu^j = 0$ and $Q^j = K^j$.

It is often more desirable to work with concentration ratios rather than activity ratios. If we define K_x^j and Q_x^j by

$$K_x^j = \frac{\gamma_f^j}{\gamma_s^j}\left(K^j\right)^{1/\nu}, \qquad Q_x^j = \frac{x_s^j}{x_f^j}, \tag{67}$$

where Q_x^j is a molar concentration ratio, then $Q_x^j = K_x^j$ in equilibrium. We can relate Q_x^j and K_x^j to the chemical potential differences by

$$\frac{Q_x^j}{K_x^j} = \left(\frac{Q^j}{K^j}\right)^{1/\nu} = \exp\left(\frac{\Delta\mu^j}{\nu R^j T}\right). \tag{68}$$

7.1 Solidus and liquidus surfaces

Since $Q_x^j = K_x^j$ in equilibrium, the equilibrium molar compositions $x^j{}_{s(eq)}$ and $x^j{}_{f(eq)}$ satisfy

$$x_{s(eq)}^j = K_x^j x_{f(eq)}^j, \quad \sum x_{s(eq)}^j = 1, \quad \sum x_{f(eq)}^j = 1. \tag{69}$$

The permissible values of $x^j{}_{s(eq)}$ and $x^j{}_{f(eq)}$ describe the solidus and liquidus surfaces, respectively.

If K_x is a function only of temperature and pressure (as is the case for an ideal solution and will be assumed from here on), the two surfaces can be described separately as follows. The solidus is given by those molar compositions $x^j{}_{s(eq)}$ satisfying

$$\sum_j \frac{x_{s(eq)}^j}{K_x^j} = 1, \qquad \sum x_{s(eq)}^j = 1 \tag{70}$$

and the liquidus is given by those molar compositions $x^j{}_{f(eq)}$ satisfying

$$\sum_j K_x^j x_{f(eq)}^j = 1, \qquad \sum x_{f(eq)}^j = 1. \tag{71}$$

Eqs (70) and (71) embody the Gibbs' phase rule: For a two-phase n-component system the phase rule states that there are n thermodynamic degrees of freedom in equilibrium. The n degrees of freedom could be T, P and $n-2$ of the components of x_s^j. In a binary system $n=2$ and the equilibrium compositions can be completely specified by T and P. The solidus is given by (70),

$$\frac{x_{s(eq)}^1}{K_x^1(P,T)} + \frac{x_{s(eq)}^2}{K_x^2(P,T)} = 1, \qquad x_{s(eq)}^1 + x_{s(eq)}^2 = 1 \tag{72}$$

and the liquidus by (71),

$$K_x^1(P,T)x_{f(eq)}^1 + K_x^2(P,T)x_{f(eq)}^2 = 1, \qquad x_{f(eq)}^1 + x_{f(eq)}^2 = 1. \tag{73}$$

In each case there are two simultaneous equations for two unknowns, which can be solved uniquely. These expressions are used to calculate the solidus and liquidus surfaces for olivine in Fig. 1.

7.2 Temperature and pressure dependence of equilibrium constants

The temperature and pressure dependence of the equilibrium constants $K^j(P, T)$ need to be prescribed. The van't Hoff equation

describes the temperature dependence

$$\frac{\partial \log K^j}{\partial T} = \frac{\Delta h^j}{R^j T^2}, \tag{74}$$

where Δh^j is the change in enthalpy for melting of pure component j. The pressure dependence is

$$\frac{\partial \log K^j}{\partial P} = -\frac{\Delta(1/\rho^j)}{R^j T}. \tag{75}$$

It is helpful to look at a simplified form of these dependencies. For example, if we assume that Δh^j is independent of temperature and pressure, then a suitable approximate expression is (Bradley 1962)

$$\log K^j = -\frac{\Delta h^j}{R^j}\left(\frac{1}{T} - \frac{1}{T_m^j(P)}\right). \tag{76}$$

$T_m^j(P)$ is the melting temperature of the pure component as a function of pressure. Recall that $\Delta h^j \equiv -L^j$, where L^j is the latent heat. In terms of K_x^j, (76) can be rewritten as

$$\log K_x^j = \log\left(\gamma_f^j/\gamma_s^j\right) - \frac{\Delta h^j}{\nu R^j}\left(\frac{1}{T} - \frac{1}{T_m^j(P)}\right). \tag{77}$$

The function $T_m^j(P)$ satisfies the Clapeyron equation,

$$\frac{\mathrm{d}T_m^j}{\mathrm{d}P} = \frac{T_m^j \Delta(1/\rho^j)}{\Delta h^j}, \tag{78}$$

which could formally be integrated to determine $T_m^j(P)$. However, it is often easier to use an approximate parameterised form for $T_m^j(P)$, such as Simon's equation,

$$T_m^j(P) = T_{m0}^j\left(1 + \frac{P}{a^j}\right)^{1/b^j}, \tag{79}$$

for some coefficients a^j and b^j. This is the approach taken here.

8 PHENOMENOLOGICAL LAWS FOR INTERPHASE MASS TRANSFER

To complete the governing equations, phenomenological laws are required describing the fluxes of mass and heat. In this section, we focus on the phenomenological laws for interphase mass transfer and the corresponding discussion for intraphase vector fluxes can be found in Section B. The simplest closure is to assume local thermodynamic equilibrium (e.g. Ribe 1985a; Hewitt & Fowler 2008; Katz 2008; Tirone *et al.* 2009). This adds n algebraic equations to the system, for example, of the form $x_s^j = K_x x_f^j$ (see 69) and constrains the solid and liquid to lie on the solidus and liquidus on the phase diagram. The interphase mass transfers are then implicitly determined. However, in this work we are interested in disequilibrium effects and thus do not assume local thermodynamic equilibrium.

According to the theory of non-equilibrium thermodynamics (de Groot & Mazur 1984), linear phenomenological laws can be obtained by examining the expression for entropy production. For example, the part of the entropy production due to transfer of components between phases is given in (42) as

$$\sigma = \sum_j \Gamma^j \frac{\Delta\mu^j}{T}. \tag{80}$$

This expression defines a natural set of conjugate thermodynamic forces ($\Delta\mu^j/T$) and fluxes (Γ^j) and suggests linear phenomenological laws of the form

$$\Gamma^j = \sum_k E^{jk}\frac{\Delta\mu^k}{T} = \sum_k E^{jk}\nu R^k \log\left(\frac{Q^k}{K^k}\right)^{1/\nu}, \tag{81}$$
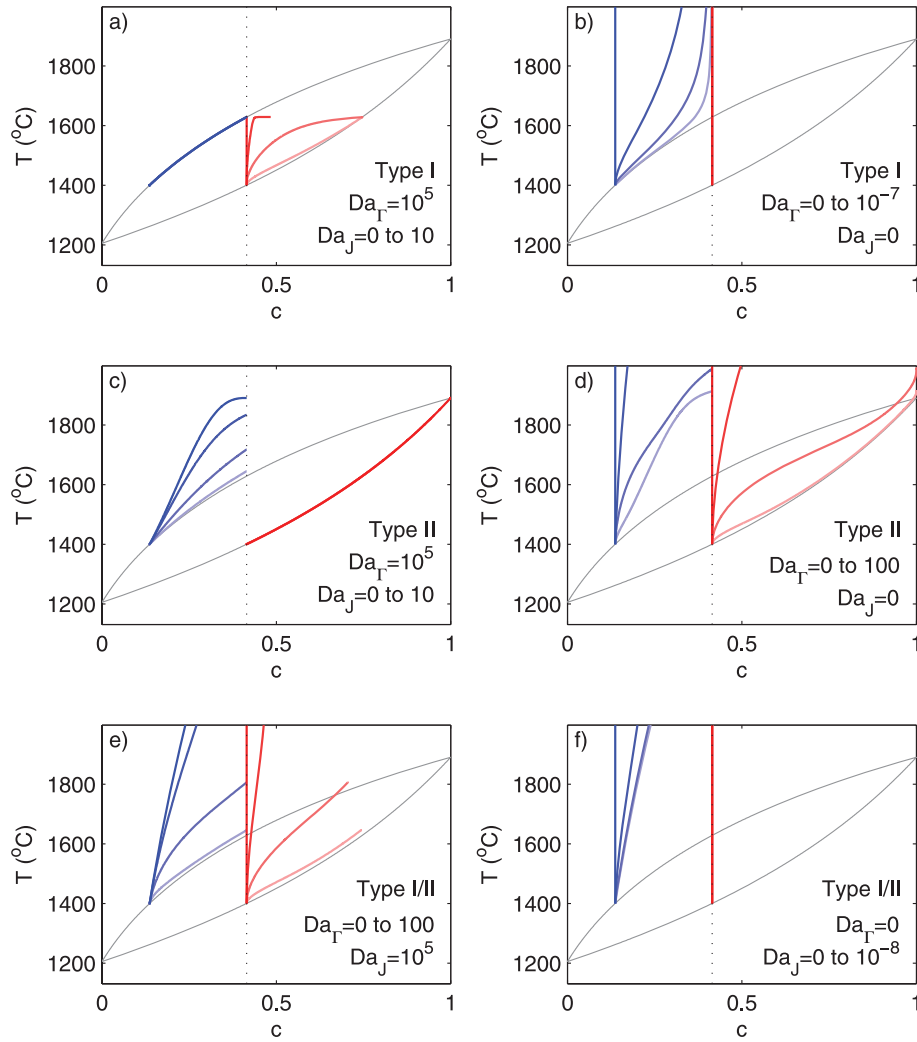
Figure 1. Examples of isobaric disequilibrium melting of olivine. Each panel is plot of temperature T against composition c. The grey lines in the background show the olivine binary phase loop (the equilibrium solidus and liquidus curves). $c = 1$ is pure forsterite, $c = 0$ is pure fayalite. The dotted line indicates the bulk composition, $c = 0.41$. Red curves show the solid composition, blue curves show the liquid composition. Each panel is for a particular style of melting (either type I or type II) for the range of Damköhler numbers indicated. In each case, dark shading indicates small Damköhler number, light shading indicates large Damköhler number. (a) and (b) are examples of type I melting, (c) and (d) are examples of type II melting and (e) and (f) are the same for both type I and type II melting (see discussion in text).

for some matrix of coefficients E^{jk}. Onsager's reciprocal relations state that E^{jk} is a symmetric matrix, $E^{jk} = E^{kj}$ and the second law ensures that E^{jk} is positive semi-definite. More precisely, the theory states that any scalar flux can depend on any scalar force in the entropy production and this could include a dependence of Γ^j on velocity field divergences. However, we will neglect such a dependence here and assume the interphase mass transfers only depend on differences in chemical potential (see Sramek *et al.* 2007, for further discussion).

Far from equilibrium, linear laws may be a poor description of the kinetics. Indeed, this is well known in the context of chemical reactions, where the law of mass action (based on products of activities) is generally a more useful phenomenological law far from equilibrium than linear laws based on the affinities (differences in chemical potential). This motivates the exploration of laws for interphase mass transfer that are non-linear in the chemical potential differences, but that must still satisfy the constraints of non-equilibrium thermodynamics near equilibrium.

Here we propose a simple non-linear law for interphase mass transfer that can be thought of as a generalisation of fractional melting. We introduce the law first and then explain why it may be reasonable. The law we propose is

$$\Gamma^j = \sum_k E^{jk} Z^k, \tag{82}$$

$$Z^k = \nu R^k \left(1 - \left(\frac{K^k}{Q^k} \right)^{1/\nu} \right) = \nu R^k \left(1 - \frac{K_x^k x_f^k}{x_s^k} \right), \tag{83}$$

which is very similar to (81). Again E^{jk} is a matrix of coefficients, which we will assume is symmetric and positive semi-definite (see Subsection 8.3 for further discussion of the second law). Z^k are the thermodynamic forces which are now given by a non-linear law in terms of the equilibrium constants K^k and activity ratios Q^k. The dependence on the ratio K^k/Q^k is found in many kinetic theories, such as transition state theory (Anderson 2005; Lasaga 1998). Near equilibrium this non-linear phenomenological law reduces to the linear law of (81), as $Z^k \approx \Delta\mu^k/T$ near equilibrium.

To make the link with fractional melting, it is useful to express the fluxes in a different way, separating out the mass flux associated with phase change (Γ) from the fluxes of components that occur without phase change (Baker & Cahn 1971; Caroli *et al.* 1986; Hillert 2006). Key to this alternative representation is the fact that the symmetric positive semi-definite matrix E^{jk} can be uniquely decomposed as

$$E^{jk} = \lambda_\Gamma c_\Gamma^j c_\Gamma^k + G^{jk}, \tag{84}$$

where $\lambda_\Gamma > 0$, c_Γ^j is a well-defined composition (i.e. it has unit sum and positive entries) and G^{jk} is a positive semi-definite matrix with zero row and column sum. The subscripts Γ on λ_Γ and c_Γ^j are to emphasise their association with the phase change, which is clearer when the phenomenological laws (82) and (83) are rewritten using (84) as

$$\Gamma^j = \Gamma c_\Gamma^j + J^j, \tag{85}$$

$$\Gamma = \lambda_\Gamma \sum_k c_\Gamma^k Z^k, \tag{86}$$

$$J^j = \sum_k G^{jk} Z^k. \tag{87}$$

Eq. (85) splits the mass flux of component j into two parts: a part that occurs due to phase change (Γc_Γ^j, since $\sum_j \Gamma c_\Gamma^j = \Gamma$) and a part that occurs without phase change (J^j, since $\sum_j J^j = 0$). The flux due to phase change is controlled by the coefficients λ_Γ (a rate constant for phase change) and c_Γ^j, whereas the flux of components that occurs without phase change is controlled by the coefficients G^{jk} since $\sum_j \sum_k G^{jk} Z^k = 0$. This decomposition into fluxes with and without phase change is useful because the different mass fluxes may be controlled by quite different physical mechanisms and thus occur at different kinetic rates.

Whether written as (82) or (85)–(87), there remains a set of $n(n+1)/2$ coefficients to be prescribed, either in the form of the $n(n+1)/2$ independent entries of the matrix E^{jk} or as λ_Γ, the $n-1$ independent entries of c_Γ^j and the $n(n-1)/2$ independent entries of G^{jk}. Either set can be specified and the other set is then determined. In this work, we will focus on two natural choices for the composition c_Γ^j and will refer to the two laws as type I and type II melting. One of these laws generalises melting laws which leave the solid composition unchanged (type I melting) and the other generalises fractional melting (type II melting).

8.1 Fractional melting (Type II melting)

During fractional melting the solid remains on the solidus and each infinitesimal increment of melt produced is in equilibrium with the solid. Once the infinitesimal melt has formed it is chemically isolated from the solid and no further chemical exchange occurs (although heat is still exchanged as thermal equilibrium is assumed). We will refer to this style of fractional melting as thermally equilibrated fractional melting (which differs from the incrementally isentropic fractional melting described by Asimow *et al.* (1997) and Stolper & Asimow (2007), which does not involve thermal equilibration).

The laws for fractional melting can be written as (Spiegelman & Elliott 1993; Spiegelman 1996)

$$\sum_k \frac{x_s^k}{K_x^k} = 1, \tag{88}$$

$$\Gamma^j = \Gamma c_\Gamma^j, \quad x_\Gamma^j = \frac{x_s^j}{K_x^j}, \tag{89}$$

where (88) constrains the solid to lie on the solidus and (89) states that the melt produced is in equilibrium with the solid. x_Γ^j represents the molar concentrations of the infinitesimal melt produced and c_Γ^j the corresponding mass concentrations (x_Γ^j and c_Γ^j are related by 58). In (89) phase change is the only form of mass transfer; comparison with (85) shows that the J^j (the fluxes of components without phase change) are all zero.

We would like to relate the laws given by (88)–(89) to those of (85)–(87). It is clear that to reproduce fractional melting the coefficients G^{jk} should be zero, but is less clear how the coefficients λ_Γ and c_Γ^j should be chosen. Eq. (89) motivates choosing the composition associated with phase change as

$$x_\Gamma^j = \left\{ \frac{x_s^j}{K_x^j} \right\} \tag{90}$$

where $\{\cdot\}$ again refers to normalising to unit sum. Note that normalisation is required, since x_s^j/K_x^j is not guaranteed to be a valid composition (i.e. sum to 1) as the solid is not necessarily constrained to the solidus for general disequilibrium phenomenological laws. The phenomenological law describing phase change (86) and (83) becomes

$$\Gamma = \lambda_\Gamma \sum_k c_\Gamma^k \nu R^k \left(1 - \frac{K_x^k x_f^k}{x_s^k} \right) \tag{91}$$

$$\propto \lambda_\Gamma \sum_k \frac{x_s^k}{K_x^k} \left(1 - \frac{K_x^k x_f^k}{x_s^k} \right) \tag{92}$$

$$\propto \lambda_\Gamma \left(\left[\sum_k \frac{x_s^k}{K_x^k} \right] - 1 \right) \tag{93}$$

and thus the constraint that the solid lies on the solidus is recovered as $\lambda_\Gamma \to \infty$. Hence fractional melting is recovered with the coefficient choice of $\lambda_\Gamma \to \infty$, $G^{jk} = 0$ and $x_\Gamma^j = \{x_s^j/K_x^j\}$. Indeed, the main reason for choosing the particular non-linear form in (83) is to exactly recover the solidus constraint, which is only approximately recovered with the linear law. We will refer to any melting law which has $x_\Gamma^j = \{x_s^j/K_x^j\}$ as type II melting. A similar generalisation can be made for fractional crystallisation and is discussed in Section C.

8.2 Solid invariant melting (Type I melting)

Another natural choice for the composition x_Γ^j is the solid composition itself, $x_\Gamma^j = x_s^j$, which we will refer to as type I melting. If the coefficients G^{jk} are zero, then this style of melting keeps the solid composition fixed. If $\lambda_\Gamma \to \infty$, this style of melting constrains the liquid to the liquidus.

The two styles of melting we consider here (type I and type II) are not the only styles of melting one could consider: they simply represent two natural choices for the composition associated with melting based on the solid composition. There is plenty of scope for further exploration of these laws.

8.3 The positivity of entropy production

The second law of thermodynamics demands that the entropy production σ is positive. For a linear phenomenological law, such as that given by (81), it is straightforward to derive conditions on the

matrix of phenomenological coefficients E^{jk} such that positive entropy production is assured. Since the entropy production (80) for a linear law is simply

$$\sigma = \frac{1}{T^2} \sum_j \sum_k E^{jk} \Delta \mu^j \Delta \mu^k, \tag{94}$$

a positive entropy production is assured for all $\Delta \mu^k$ if and only if E^{jk} is a positive semi-definite matrix.

With non-linear phenomenological laws the situation is not so straightforward: even if E^{jk} is a positive definite matrix, it is not necessarily the case that the resulting entropy production is positive and other constraints must be placed on the coefficients E^{jk}. For the melting laws given by (82) and (83), the entropy production (80) can be written in terms of chemical potentials as

$$\sigma = \sum_j \sum_k E^{jk} \nu R^k \left(1 - \exp \left(-\frac{\Delta \mu^k}{\nu R^k T} \right) \right) \frac{\Delta \mu^j}{T}, \tag{95}$$

or more simply as

$$\sigma = \sum_j \sum_k E^{*jk} \left(1 - e^{-d^k} \right) d^j, \tag{96}$$

where $d^j = \Delta \mu^j / \nu R^j T$ and $E^{*jk} = \nu^2 R^j R^k E^{jk}$. If (96) could be linearised $1 - e^{-d^k} \approx d^k$, then the entropy production is assured to be positive if E^{*jk} is a positive semi-definite matrix. But for the general non-linear law, having E^{*jk} be a positive semi-definite matrix is not enough to guarantee positive entropy production.

There are certain simple forms for E^{*jk} that will guarantee a positive entropy production for the non-linear law. For example, if E^{*jk} is diagonal, with positive entries on the diagonal, then the entropy production is positive because the function $f(x) = x(1 - e^{-x})$ is always positive. If $E^{*jk} = \lambda c^j c^k$ for some composition c^j and constant $\lambda > 0$, then the entropy production will be positive provided all the d^j have the same sign, since the two quantities $\sum_j c^j d^j$ and $\sum_k c^k (1 - e^{-d^k})$ are then either both positive or both negative. Having all the d^j the same sign is a common occurrence and is true for the example calculations throughout this work. For a binary system the entropy production is always positive for arbitrary positive semi-definite matrices E^{*jk} when the d^j have the same sign, because matrices of the form in (97) also always give a positive entropy production (recall the decomposition in 84). For more general cases, the positivity of the entropy production with this non-linear law can not be taken for granted. If the d^j differ in sign the entropy production may go negative with the present non-linear law: this implies other non-linear laws are needed to describe such circumstances and must be developed.

9 ISOBARIC BINARY MELTING

As a concrete example in which to explore the behaviour of these phenomenological laws, we now consider the problem of isobaric melting of olivine. Our model olivine is a complete solid solution of two components, forsterite (Mg_2SiO_4) and fayalite (Fe_2SiO_4), with a simple binary loop phase diagram. For a binary system the matrix G^{jk} has only one free parameter and takes the form

$$G^{jk} = \lambda_J \begin{pmatrix} 1 & -1 \\ -1 & 1 \end{pmatrix}, \tag{97}$$

where $\lambda_J > 0$. In full, the phenomenological laws for melting are thus

$$Q_x^1 = \frac{x_s}{x_f}, \qquad Q_x^2 = \frac{1 - x_s}{1 - x_f}, \tag{98}$$

$$K_x^1 = \exp \left(\frac{L^1}{\nu R^1} \left(\frac{1}{T} - \frac{1}{T_m^1(P)} \right) \right), \tag{99}$$

$$K_x^2 = \exp \left(\frac{L^2}{\nu R^2} \left(\frac{1}{T} - \frac{1}{T_m^2(P)} \right) \right), \tag{100}$$

$$T_m^1(P) = T_{m0}^1 \left(1 + \frac{P}{a^1} \right)^{1/b^1}, \qquad T_m^2(P) = T_{m0}^2 \left(1 + \frac{P}{a^2} \right)^{1/b^2}, \tag{101}$$

$$Z^1 = \nu R^1 \left(1 - \frac{K_x^1}{Q_x^1} \right), \qquad Z^2 = \nu R^2 \left(1 - \frac{K_x^2}{Q_x^2} \right), \tag{102}$$

$$\Gamma = \lambda_\Gamma \left(c_\Gamma Z^1 + (1 - c_\Gamma) Z^2 \right), \tag{103}$$

$$J = \lambda_J \left(Z^2 - Z^1 \right), \tag{104}$$

$$\Gamma^1 = c_\Gamma \Gamma - J, \tag{105}$$

$$\Gamma^2 = (1 - c_\Gamma) \Gamma + J, \tag{106}$$

where the composition variable x refers to the molar concentration of component 1 (forsterite): the molar concentration of component 2 (fayalite) is $1 - x$. Numerical values for model olivine parameters can be found in Table 1. Note that the kinetic rates $\lambda_\Gamma, \lambda_J > 0$ to satisfy the second law. λ_Γ and λ_J could depend on many variables such as temperature or porosity, but for simplicity, here λ_Γ and λ_J will be assumed constant.

For type I melting,

$$x_\Gamma = x_s, \tag{107}$$

whereas for type II melting,

$$x_\Gamma = \frac{x_s / K_x^1}{x_s / K_x^1 + (1 - x_s) / K_x^2}. \tag{108}$$

Consider heating a piece of olivine at fixed pressure such that its temperature rises at a constant rate. Let F be the mass fraction of melt (initially zero). The evolution of F and composition c_f are described by

$$\frac{dF}{dt} = \frac{\Gamma}{\rho_0}, \tag{109}$$

$$\frac{d(Fc_f)}{dt} = \frac{\Gamma^1}{\rho_0}, \tag{110}$$

where ρ_0 is the initial density of the unmelted solid. In non-dimensional form this simple system can be described in terms of temperature as

$$\frac{dF}{dT} = \Gamma, \tag{111}$$

$$\frac{d(Fc_f)}{dT} = \Gamma^1, \tag{112}$$

$$Z^1 = 1 - \frac{K_x^1}{Q_x^1}, \qquad Z^2 = \frac{R^2}{R^1} \left(1 - \frac{K_x^2}{Q_x^2} \right), \tag{113}$$

$$\Gamma = Da_\Gamma \left(c_\Gamma Z^1 + (1 - c_\Gamma) Z^2 \right), \tag{114}$$

$$J = Da_J \left(Z^2 - Z^1 \right), \tag{115}$$

Table 1. Approximate parameters for the forsterite–fayalite binary system, $(MgFe)_2SiO_4$. There are two atoms of (Mg,Fe) per formula unit and thus $\nu = 2$. The latent heats are chosen to match the phase diagram using the parametrisation of Bradley (1962), although here the specific heat capacities are assumed identical for solid and liquid. The melting temperature as a function of temperature has been parametrised by Simon's equation. Thermal expansion coefficients are assumed identical for the two components.

		$j = 1$: Forsterite	$j = 2$: Fayalite	Notes
Formula		Mg_2SiO_4	Fe_2SiO_4	
Latent heat of fusion	L^j	8.71×10^5 J kg^{-1}	5.17×10^5 J kg^{-1}	Bradley (1962)
Melting temperature	T^j_{m0}	2163 K	1478 K	at 0.1 MPa, Bradley (1962)
Simon's equation coefficient	a^j	10.83 GPa	15.78 GPa	Bottinga (1985), Poirier (2000)
Simon's equation coefficient	b^j	3.70	1.59	Bottinga (1985), Poirier (2000)
Molar mass	M^j	0.1406934 kg mol^{-1}	0.2037736 kg mol^{-1}	
Specific gas constant	R^j	59.096 J K^{-1} kg^{-1}	40.803 J K^{-1} kg^{-1}	
Solid density	ρ^j_s	3222 kg m^{-3}	4392 kg m^{-3}	Deer *et al.* (1992)
Melt density	ρ^j_f	3053 kg m^{-3}	4026 kg m^{-3}	Calculated from Clapeyron relation
Solid thermal expansion coefficient	α^j_s	2.6×10^{-5}K^{-1}	2.6×10^{-5}K^{-1}	Fa at 298-1123 K, Ahrens (1995)
Melt thermal expansion coefficient	α^j_f	4.8×10^{-5}K^{-1}	4.8×10^{-5}K^{-1}	Fa at 1573-1873 K, Agee (1992)
Specific heat capacity	C^j	1.3×10^3 J K^{-1} kg^{-1}	1.3×10^3 J K^{-1} kg^{-1}	Fo at 1500 K, Ahrens (1995)

$$\Gamma^1 = c_\Gamma \Gamma - J, \tag{116}$$

where the temperature has been non-dimensionalised by a typical temperature scale ΔT, taken here to be the difference between the melting points of the two components $\Delta T = T^1_m - T^2_m$. The mass exchanges Γ and Γ^1 are non-dimensionalised on $\Delta T/(\rho_0 dT/dt)$, where dT/dt is the (assumed constant) rate of temperature increase. The behaviour of this simple system is determined by two non-dimensional Damköhler numbers,

$$Da_\Gamma = \frac{\lambda_\Gamma \nu R^1 \Delta T}{\rho_0 (dT/dt)}, \qquad Da_J = \frac{\lambda_J \nu R^1 \Delta T}{\rho_0 (dT/dt)}, \tag{117}$$

which are ratios of the kinetic rates to the rate at which the temperature increases.

Fig. 1 gives examples of the different styles of disequilibrium melting that occur as the two Damköhler numbers are varied for the two types of melting. If both Damköhler numbers are large, $Da_\Gamma \to \infty$ and $Da_J \to \infty$, the kinetic rates are much faster than the rate at which the temperature increases and thus the melting occurs in equilibrium (batch melting). In equilibrium, the solid composition lies on the solidus and the liquid composition lies on the liquidus. Equilibrium melting begins when the bulk composition intersects the solidus and completes when the bulk composition intersects the liquidus. To avoid a singularity near the onset of melting, the calculations of Fig. 1 assume there is initially a very small melt fraction ($F = 10^{-10}$) present before melting begins with a composition in equilibrium with the solid.

Fig. 1(a) shows the effect of reducing Da_J while keeping Da_Γ large for type I melting. Since Da_Γ is large the liquid composition remains on the liquidus (the constraint imposed by type I melting). But the solid composition deviates the solidus: in the end-member case of $Da_J = 0$ (dark shading), the solid composition is invariant with changing temperature (since $\Gamma^j = \Gamma c^j_s$ in this limit). With small Da_J and large Da_Γ, the lever rule (conservation of mass) implies that there is little melting until the bulk composition comes close to crossing the liquidus.

Fig. 1(b) shows the effect of then reducing Da_Γ while keeping $Da_J = 0$ for type I melting. With Da_Γ large, the situation is the same as seen in Fig. 1a with the solid invariant and the liquid on the liquidus. The solid remains invariant as Da_Γ is varied (since $Da_J = 0$ and thus $\Gamma^j = \Gamma c^j_s$) and for the end member case of $Da_\Gamma = Da_J = 0$ (dark shading) there is no mass transfer whatsoever and both liquid and solid composition remain invariant with increasing temperature.

Fig. 1(c) is perhaps the most important of the panels in Fig. 1 and demonstrates the transition from batch to fractional melting, showing type II melting for large Da_Γ and a range of Da_J. The large Da_Γ constrains the solid to the solidus (the constraint imposed by type II melting), but the liquid composition deviates from the liquidus as Da_J is reduced. The end member case of $Da_J = 0$ (dark shading) is essentially the fractional melting path (e.g. Maaløe 1984). The corresponding melt production for this case is shown in Fig. 2, which can be determined from Fig. 1(c) using the lever rule.
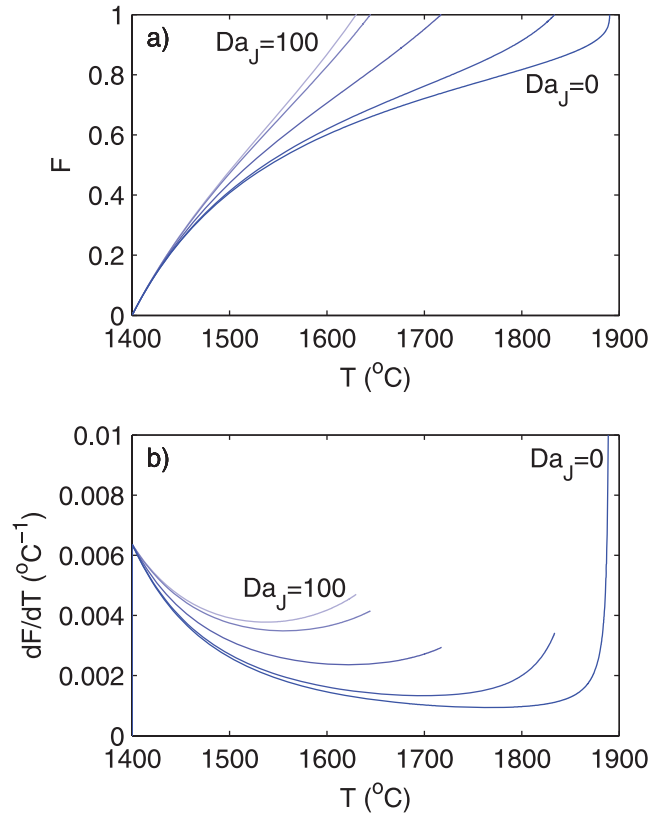

Figure 2. (a) Mass fraction of melt F as a function of temperature T for type II isobaric melting with $Da_\Gamma = 10^5$ and varying Da_J (see Fig. 1c, and also Fig. 5 of Asimow *et al.* 1997). (b) Corresponding isobaric melt productivity dF/dT.

Fig. 1(d) shows the effect of then reducing Da_Γ while keeping $Da_J = 0$ for type II melting. With Da_Γ large, the situation is the same as seen in Fig. 1(a) with the solid on the solidus and the liquid following the fractional melting path. Similar to Fig. 1(b), for the end member case of $Da_\Gamma = Da_J = 0$ (dark shading) there is no mass transfer whatsoever and both liquid and solid composition remain invariant with increasing temperature.

Figs 1(e) and (f) demonstrate situations that are essentially independent of the choice of c_Γ and thus the same for both type I and type II melting. Fig. 1e has Da_J large and thus there is the approximate constraint that $Z^1 = Z^2$ and hence $\Gamma = \lambda_\Gamma Z^1$, independent of c_Γ. With Da_Γ large the situation is essentially batch melting, while the other end member of $Da_\Gamma = 0$ (dark shading) has no melting, although the solid and liquid can still exchange components without phase change. Since the initial melt fraction is exceedingly small ($F = 10^{-10}$) the solid composition is buffered and is invariant as the temperature is increased, while the liquid composition undergoes a notable shift.

Fig. 1(f) has $Da_\Gamma = 0$ and thus no melting ($\Gamma = 0$). Hence $\Gamma^1 = -\Gamma^2 = \lambda_J(Z^2 - Z^1)$ independent of the choice of c_Γ. For large Da_J the situation is the same as that seen in Fig. 1(e), with an invariant solid composition and a shifting liquid composition. For the other end member case of $Da_\Gamma = Da_J = 0$ (dark shading) there is once again no mass transfer whatsoever, with both liquid and solid composition remaining invariant with increasing temperature.

10 1-D BINARY MELTING COLUMN

One of the simplest problems combining compaction and melting is the 1-D steady state melting column. The problem was first addressed using the McKenzie (1984) equations by Ribe (1985a) and has since been studied by many other authors (Asimow & Stolper 1999; Spiegelman & Elliott 1993; Sramek *et al.* 2007; Hewitt & Fowler 2008; Katz 2008). Here we investigate the effects of disequilibrium on this problem. Again we consider melting of pure olivine, although it should be noted that real mantle melting involves a multiphase assemblage of a number of minerals. Olivine is the most abundant mantle mineral by mass, but it is not the mineral that melts most during real mantle melting. Nevertheless it provides a simple binary test system for studying the behaviour of the equations.

In 1-D, with no diffusion of heat or components, the conservation eqs (1), (2), (9), (10), (29), (30) and (53) are

$$\frac{d}{dz}\left(\phi \rho_f v_f\right) = \Gamma, \tag{118}$$

$$\frac{d}{dz}\left((1 - \phi)\rho_s v_s\right) = -\Gamma, \tag{119}$$

$$\frac{d}{dz}\left(\phi \rho_f v_f c_f\right) = \Gamma^1, \tag{120}$$

$$\frac{d}{dz}\left((1 - \phi)\rho_s v_s c_s\right) = -\Gamma^1, \tag{121}$$

$$\frac{dP}{dz} = -\overline{\rho}g - \frac{d\tilde{P}}{dz}, \tag{122}$$

$$\frac{d\tilde{P}}{dz} = \frac{\mu}{k_\phi}\phi\left(v_f - v_s\right) - (1 - \phi)\Delta\rho g, \tag{123}$$

$$\frac{dv_s}{dz} = \frac{-\tilde{P}}{\zeta_\phi + \frac{4}{3}\eta_\phi}, \tag{124}$$

$$\overline{\rho C v}\frac{dT}{dz} = T\overline{\alpha v}\frac{dP}{dz} - \Gamma^1 L^1 - \Gamma^2 L^2, \tag{125}$$

where the viscous dissipation term Ψ has been neglected in the energy eq. (125) (see Asimow 2002, for justification). The quantity $\tilde{P}$ is a compaction pressure, defined by $-\overline{\sigma}_{zz} = P + \tilde{P}$. c_f and c_s are the concentrations by mass of component 1: the concentrations of component 2 are given by $c_f^2 = 1 - c_f, c_s^2 = 1 - c_s$. Constitutive laws for viscosities and permeabilities are assumed to take the simplified forms

$$\zeta_\phi + \frac{4}{3}\eta_\phi = \left(\zeta_0 + \frac{4}{3}\eta_0\right)\phi^{-m}, \tag{126}$$

$$k_\phi = k_0\phi^n, \tag{127}$$

where the typical choices of the exponents are $m = 1$ (Simpson *et al.* 2010a) and $n = 3$ (Kozeny–Carman equation). The above eqs (118)–(127) together with the phenomenological laws for melting (98)–(106) form a closed set of governing equations.

Most of the boundary conditions for this problem are at the onset of melting: the incoming material there has zero porosity, density ρ_0, upwelling velocity v_0 and composition c_0. T and P are chosen such that the system is initially at the onset of melting (either T or P can be set and the other is then determined from the solidus). The final boundary condition concerns the momentum equations and we choose $d\tilde{P}/dz = 0$ on the top boundary (a free flux condition Spiegelman (1993a); see Sramek *et al.* (2007) and Hewitt & Fowler (2008) for further discussion of possible boundary conditions).

Conservation of mass places strong constraints on 1-D steady state melting (Ribe 1985a; Spiegelman & Elliott 1993; Asimow & Stolper 1999). On summing (118) and (119) and integrating, we have

$$\phi \rho_f v_f + (1 - \phi)\rho_s v_s = \rho_0 v_0. \tag{128}$$

Similarly, from (120) and (121),

$$\phi \rho_f c_f v_f + (1 - \phi)\rho_s c_s v_s = \rho_0 c_0 v_0. \tag{129}$$

The governing eqs (118)–(127) can be simplified by introducing the degree of melting F, which can be defined as a ratio of melt flux to incoming mass flux,

$$F = \frac{\phi \rho_f v_f}{\rho_0 v_0}, \tag{130}$$

where $F = 0$ at the onset of melting and $F = 1$ once melting is complete. It follows from (128)–(130) that

$$Fc_f + (1 - F)c_s = c_0. \tag{131}$$

In the case of equilibrium melting, the conservation of energy equation implies that total entropy flux is conserved along the column and a similar equation to (131) can be written for entropy (i.e. $Fs_f + (1 - F)s_s = s_0$, Asimow & Stolper 1999). The isentropic nature of the equilibrium process simplifies the analysis greatly (Asimow *et al.* 1997; Asimow & Stolper 1999; Stolper & Asimow 2007). However, when there is disequilibrium between the two phases, there is the potential for entropy production and we cannot make this simplification here.

In terms of F, the governing eqs (118)–(127) are

$$\frac{dF}{dz} = \frac{\Gamma}{\rho_0 v_0}, \tag{132}$$

$$\frac{\mathrm{d}m}{\mathrm{d}z} = \frac{\Gamma^1}{\rho_0 v_0}, \tag{133}$$

$$\frac{\mathrm{d}P}{\mathrm{d}z} = -\bar{\rho}g - \frac{\mathrm{d}\tilde{P}}{\mathrm{d}z}, \tag{134}$$

$$\frac{\mathrm{d}\tilde{P}}{\mathrm{d}z} = \frac{\mu}{k_\phi}q - (1-\phi)\,\Delta\rho g, \tag{135}$$

$$\frac{\mathrm{d}v_s}{\mathrm{d}z} = \frac{-\tilde{P}}{\zeta_\phi + \frac{4}{3}\eta_\phi}, \tag{136}$$

$$\left(FC_f + (1-F)C_s\right)\frac{\mathrm{d}T}{\mathrm{d}z}$$
$$= T\left(F\frac{\alpha_f}{\rho_f} + (1-F)\frac{\alpha_s}{\rho_s}\right)\frac{\mathrm{d}P}{\mathrm{d}z} - \frac{\Gamma^1 L^1}{\rho_0 v_0} - \frac{\Gamma^2 L^2}{\rho_0 v_0}, \tag{137}$$

where $m = Fc_f$ is the mass of component 1 in the fluid phase. The notation $q = \phi\left(v_f - v_s\right)$ is used to signify the Darcy flux. Conservation of mass (128)–(131) implies

$$v_s = \frac{\rho_0 v_0(1-F)}{\rho_s(1-\phi)}, \quad q = F\frac{\rho_0 v_0}{\rho_f} + (1-F)\frac{\rho_0 v_0}{\rho_s} - v_s, \tag{138}$$

$$c_f = \frac{m}{F}, \quad c_s = \frac{c_0 - m}{1 - F}. \tag{139}$$

Formally the densities ρ_s and ρ_f could vary as a function of temperature, pressure and composition. In practice, these variations are slight (i.e. much less than the difference in density between the two phases) and can be neglected with the exception of the adiabatic term in the energy equation. Thus we approximate ρ_s and ρ_f as constants in the equations to follow. Since we assume initial zero porosity, $\rho_0 = \rho_s$. We will assume that the specific heat capacities of solid and fluid are constant and equal and thus on the left hand side of (137), $FC_f + (1-F)\,C_s = C$.

10.1 Non-dimensionalisation

For numerical solution and further analysis it is helpful to non-dimensionalise the equations. If Δz is a typical length scale (e.g. the height of the melting column) and ΔT is a typical temperature scale (e.g. the difference in melting temperatures ($\Delta T = T_m^1 - T_m^2$), then we can non-dimensionalise as $z = z'\Delta z$, $T = T'\Delta T$, $P = P'\rho_s g\Delta z$, $\tilde{P} = \tilde{P}'(\zeta_0 + \frac{4}{3}\eta_0)v_0/\Delta z$, $\Gamma = \Gamma'\rho_s v_0/\Delta z$, $V = V'v_0$, $q = q'v_0$, etc. The following non-dimensional parameters control the behaviour of the system:

$$\mathcal{A} = \frac{\alpha_s g\Delta z}{C}, \quad \mathcal{B} = \frac{k_0\Delta\rho g}{\mu v_0}, \quad \mathcal{C} = \frac{k_0\left(\zeta_0 + \frac{4}{3}\eta_0\right)}{\mu(\Delta z)^2}, \tag{140}$$

$$r_\alpha = \frac{\alpha_f}{\alpha_s}, \quad r_\rho = \frac{\rho_f}{\rho_s}, \tag{141}$$

$$\mathcal{R}^1 = \frac{\nu R^1}{C}, \quad \mathcal{R}^2 = \frac{\nu R^2}{C}, \tag{142}$$

$$\mathrm{St}^1 = \frac{L^1}{C\Delta T}, \quad \mathrm{St}^2 = \frac{L^2}{C\Delta T}, \tag{143}$$

$$\mathrm{Da}_\Gamma = \frac{\lambda_\Gamma \nu R^1 \Delta z}{\rho_s v_0}, \quad \mathrm{Da}_J = \frac{\lambda_J \nu R^1 \Delta z}{\rho_s v_0}. \tag{144}$$

Table 2. Non-dimensional parameters used in the 1-D melting column calculations of Fig. 4 (defined in 140–144).

Adiabatic parameter	$\mathcal{A}$	0.012
Buoyancy parameter	$\mathcal{B}$	49,000
Compaction parameter	$\mathcal{C}$	260
Expansivity ratio	r_α	1.8
Density ratio	r_ρ	0.98
Specific gas constant/ specific heat capacity	$\mathcal{R}^1$	0.091
Specific gas constant/ specific heat capacity	$\mathcal{R}^2$	0.063
Stefan number	St^1	0.98
Stefan number	St^2	0.58
Damköhler number	Da_Γ	50
Damköhler number	Da_J	0 or 50

Table 3. Dimensional parameters used in the 1-D melting column calculations of Fig. 4.

Acceleration due to gravity	g	9.8 m s^{-2}
Permeability coefficient	k_0	10^{-7} m^2
Permeability exponent	n	3
Fluid viscosity	μ	1 Pa s
Bulk viscosity coefficient	$\zeta_0 + \frac{4}{3}\eta_0$	10^{19} Pa s
Bulk viscosity exponent	m	1
Upwelling velocity	v_0	50 mm yr^{-1}
Bulk composition	c_0	0.9

$\mathcal{A}$ is an adiabatic parameter, which is the product of the adiabatic gradient and the column length scale (sometimes termed the dissipation number). $\mathcal{B}$ is a buoyancy parameter, which is essentially a ratio of percolation velocity to upwelling velocity, although the ϕ dependence is missing. $\mathcal{C}$ is a compaction parameter, a ratio of compaction length squared to column length squared. The inverse of $\mathcal{C}$ is sometimes referred to as a melt retention number (Tackley & Stevenson 1993). r_α is a ratio of expansivities and r_ρ a ratio of densities. $\mathcal{R}^1$ and $\mathcal{R}^2$ are ratios of specific gas constants to specific heat capacity. St$_1$ and St$_2$ are Stefan numbers, which are a ratio of latent heat to sensible heat for the two components. Finally, Da$_\Gamma$ and Da$_J$ are Damköhler numbers, which are a ratio of reaction rates to upwelling rates.

Values of the non-dimensional parameters used in the calculations are given in Table 2, based on dimensional parameters in Tables 1 and 3. The adiabatic parameter $\mathcal{A}$ is small, which justifies the neglect of the adiabatic term by some authors (Sramek *et al.* 2007). The buoyancy parameter $\mathcal{B}$ is very large which indicates that the melt velocities will be much larger than the mean upwelling velocity. The density ratio r_ρ is close to 1, which some authors exploit by making a Boussinesq approximation (Ribe 1985a), although we do not do this here.

The Damköhler numbers used in the calculations are designed to demonstrate the effects of disequilibrium rather than necessarily being realistic. The Damköhler numbers depend on the melting kinetics at small scales, which are poorly understood. A crude order of magnitude estimate can be obtained by assuming that the melting kinetics are controlled by diffusion into the solid grains. A typical estimate of the diffusion coefficient for Fe–Mg exchange in olivine is $\sim 10^{-16}$ m^2 s^{-1} (Chakraborty 1997). For a typical grain size of 1 mm, this implies a kinetic rate of $\sim 10^{-10}$ s^{-1}. For a 60 km melting column and an upwelling rate of 50 mm yr^{-1}, this implies a Damköhler number $\sim 4'000$. This is large and suggests that the two phases should be close to equilibrium throughout the melting column. However, the disequilibrium calculations we perform use somewhat smaller Damköhler numbers so that the effects of disequilibrium can be shown.

The non-dimensional parameters $\mathcal{A}$, $\mathcal{B}$ and $\mathcal{C}$ are related to the natural length scales

$$\delta_a = \frac{\mathcal{C}}{\alpha g} = \mathcal{A}^{-1}\Delta z, \tag{145}$$

$$\delta_c = \sqrt{\frac{k_\phi(\zeta_\phi + \frac{4}{3}\eta_\phi)}{\mu}} = \phi^{(n-m)/2}\mathcal{C}^{1/2}\Delta z, \tag{146}$$

$$\delta_r = \sqrt{\frac{v_0(\zeta_\phi + \frac{4}{3}\eta_\phi)}{\Delta\rho g}} = \phi^{-m/2}\left(\frac{\mathcal{C}}{\mathcal{B}}\right)^{1/2}\Delta z, \tag{147}$$

where δ_a is the adiabatic length, δ_c is the compaction length (McKenzie 1984) and δ_r is the reduced compaction length (Ribe 1985b).

In non-dimensional form, the governing equations are

$$\frac{\mathrm{d}F}{\mathrm{d}z} = \Gamma, \tag{148}$$

$$\frac{\mathrm{d}m}{\mathrm{d}z} = \Gamma^1, \tag{149}$$

$$\frac{\mathrm{d}P}{\mathrm{d}z} = -1 + (1-r_\rho)\phi - (1-r_\rho)\frac{\mathcal{C}}{\mathcal{B}}\frac{\mathrm{d}\tilde{P}}{\mathrm{d}z}, \tag{150}$$

$$\frac{\mathrm{d}\tilde{P}}{\mathrm{d}z} = \frac{\phi^{-n}q}{\mathcal{C}} - \frac{\mathcal{B}}{\mathcal{C}}(1-\phi), \tag{151}$$

$$\frac{\mathrm{d}v_s}{\mathrm{d}z} = -\phi^m\tilde{P}, \tag{152}$$

$$\frac{\mathrm{d}T}{\mathrm{d}z} = \mathcal{A}\left(\frac{r_\alpha}{r_\rho}F + 1 - F\right)T\frac{\mathrm{d}P}{\mathrm{d}z} - \Gamma^1\mathrm{St}^1 - \Gamma^2\mathrm{St}^2, \tag{153}$$

with

$$v_s = \frac{1-F}{1-\phi}, \quad q = \frac{F}{r_\rho} + 1 - F - v_s, \quad c_f = \frac{m}{F}, \quad c_s = \frac{c_0 - m}{1-F}. \tag{154}$$

At the onset of melting (say $z = 0$) we have $F = 0$, $m = 0$, $v_s = 1$ and T and P at some given values on the solidus with composition c_0. At the surface ($z = 1$) we have $\mathrm{d}\tilde{P}/\mathrm{d}z = 0$. This is a two point boundary value problem. The governing equations are completed by the non-dimensional phenomenological laws for melting from (98)–(106),

$$Q_x^1 = \frac{x_s}{x_f}, \qquad Q_x^2 = \frac{1-x_s}{1-x_f}, \tag{155}$$

$$K_x^1 = \exp\left(\frac{\mathrm{St}^1}{\mathcal{R}^1}\left(\frac{1}{T} - \frac{1}{T_m^1(P)}\right)\right), \tag{156}$$

$$K_x^2 = \exp\left(\frac{\mathrm{St}^2}{\mathcal{R}^2}\left(\frac{1}{T} - \frac{1}{T_m^2(P)}\right)\right), \tag{157}$$

$$T_m^1(P) = T_{m0}^1\left(1 + \frac{P}{a^1}\right)^{1/b^1}, \qquad T_m^2(P) = T_{m0}^2\left(1 + \frac{P}{a^2}\right)^{1/b^2}, \tag{158}$$

$$Z^1 = 1 - \frac{K_x^1}{Q_x^1}, \qquad Z^2 = \frac{\mathcal{R}^2}{\mathcal{R}^1}\left(1 - \frac{K_x^2}{Q_x^2}\right), \tag{159}$$

$$\Gamma = \mathrm{Da}_\Gamma\left(c_\Gamma Z^1 + (1-c_\Gamma)Z^2\right), \tag{160}$$

$$J = \mathrm{Da}_J\left(Z^2 - Z^1\right), \tag{161}$$

$$\Gamma^1 = c_\Gamma\Gamma - J, \tag{162}$$

$$\Gamma^2 = (1-c_\Gamma)\Gamma + J, \tag{163}$$

$$x_\Gamma = \frac{x_s/K_x^1}{x_s/K_x^1 + (1-x_s)/K_x^2}. \tag{164}$$

Here T_{m0}^1 and T_{m0}^2 are the non-dimensional melting temperatures and the Simon's equation coefficients a^1 and a^2 are non-dimensionalised on the appropriate pressure scale.

10.2 Zero compaction length approximation

Perhaps the most important simplification to these equations that can be made is to assume $\mathcal{C} = 0$, that is, zero compaction length (Ribe 1985a; Spiegelman 1993a,b) (termed the Darcy approximation by Sramek *et al.* 2007). Formally, this is a singular perturbation of these equations, and by setting $\mathcal{C} = 0$ the compaction boundary layers are neglected. However, the problem is then a more straightforward initial value problem, with boundary conditions only specified at the onset of melting. Essentially, (150), (151) and (152) are replaced by

$$\frac{\mathrm{d}P}{\mathrm{d}z} = -1 + (1-r_\rho)\phi, \tag{165}$$

$$0 = \phi^{-n}q - \mathcal{B}(1-\phi). \tag{166}$$

Combining (166) with (154) leads to an algebraic equation for the porosity ϕ (Ribe 1985a; Spiegelman & Elliott 1993)

$$\mathcal{B}\phi^n(1-\phi)^2 + (1-F)\phi - \frac{F}{r_\rho}(1-\phi) = 0. \tag{167}$$

The zero compaction length approximation is the leading order outer solution for the full problem and is a good approximation for $\mathcal{B}$ sufficiently small and at points far away from the boundaries. This is essentially the approximation used in the original study of Ahern & Turcotte (1979). With this approximation, the disequilibrium only affects the porosity ϕ through changes in the degree of melting F.

The matrix is usually assumed sufficiently permeable that the porosity ϕ remains small throughout the melting column ($\phi \ll 1$). With small porosities, (165) and (166) can be approximated by

$$\frac{\mathrm{d}P}{\mathrm{d}z} = -1, \tag{168}$$

$$q = \mathcal{B}\phi^n, \tag{169}$$

that is, the fluid pressure is approximately lithostatic and the fluid is simply driven by its buoyancy. The 1-D melting column problem then simply consists of solving for T, F and m as a function of pressure P. For large values of the Damköhler number the problem becomes stiff and a stiff ODE solver was used to calculate numerical solutions. Examples of such solutions are shown in Fig. 3. In the limit of infinite Damköhler number (equilibrium), the equations become differential-algebraic in nature, but are still amenable to solution by stiff ODE solvers.

Fig. 3 provides examples of near-equilibrium ($\mathrm{Da}_\Gamma = 10^4$, $\mathrm{Da}_J = 10^4$) and near-fractional ($\mathrm{Da}_\Gamma = 10^4$, $\mathrm{Da}_J = 0$) melting (dotted
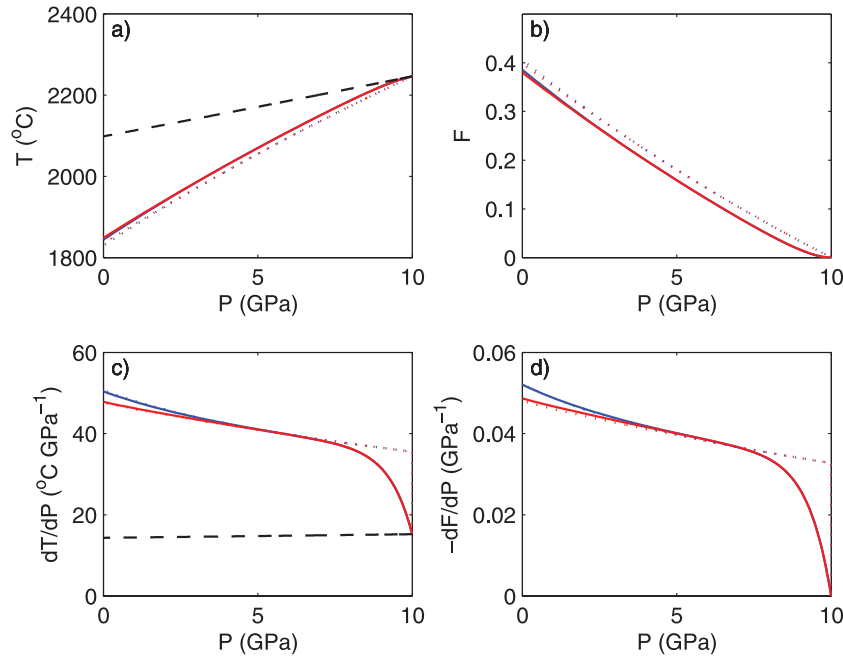
Figure 3. Type II decompression melting for $\mathrm{Da}_\Gamma = 10$, $\mathrm{Da}_J = 10$ (solid blue line) and $\mathrm{Da}_\Gamma = 10$, $\mathrm{Da}_J = 0$ (solid red line). Melting starts at 10 GPa (higher than for real mantle melting—chosen for emphasis of the differences) with a bulk composition of 0.9. There is a notable reactive boundary layer at the onset of melting. Dotted lines show near-equilibrium (blue, $\mathrm{Da}_\Gamma = 10^4$, $\mathrm{Da}_J = 10^4$) and near-fractional (red, $\mathrm{Da}_\Gamma = 10^4$, $\mathrm{Da}_J = 0$) paths for comparison. (a) Temperature versus pressure. Dashed line shows the solid adiabat. (b) Degree of melting versus pressure. (c) dT/dP versus pressure. Dashed line shows the solid adiabatic gradient. (d) Melt productivity ($-dF/dP$) versus pressure. Near-equilibrium melting has a slightly higher productivity than near-fractional melting.

lines). There is very little difference between the two cases, with near-fractional melting showing a slightly lower melt productivity ($-dF/dP$) and lower temperature drop (dT/dP) than near-equilibrium melting. In both cases, melt productivity increases with decreasing pressure, which is expected. The increase in melt productivity with decreasing pressure has been discussed in some detail by Asimow *et al.* (1997), although it should be noted that here the latent heats are assumed constant while Asimow *et al.* (1997) have latent heats increasing with T (they assumed a constant entropy jump).

The difference between fractional and equilibrium melting is much less pronounced here than seen in other studies, such as those which consider incrementally isentropic fractional fusion (Asimow *et al.* 1997; Stolper & Asimow 2007). The thermally equilibrated fractional melting considered here is fundamentally different from incrementally isentropic fractional fusion because here the two phases are always assumed to be in thermal equilibrium and thus at the same temperature. In incrementally isentropic fractional fusion each increment of melt is produced in an isentropic step and then removed from the system. However, if each increment of melt were brought to surface pressures isentropically then each increment would be at a different temperature and thus not in thermal equilibrium with the other increments. Thus these two types of fractional melting will have slightly different melt productivities.

There is a small entropy production associated with the thermally equilibrated fractional melting considered here. Recall that the part of the entropy production due to interphase transfer is

$$\sigma = \sum_j \Gamma^j \frac{\Delta\mu^j}{T}. \tag{170}$$

For fractional melting,

$$\Gamma^j = \Gamma c_\Gamma^j, \qquad \sum_j c_\Gamma^j \left(1 - \exp\left(-\frac{\Delta\mu^j}{\nu R^j T}\right)\right) = 0 \tag{171}$$

Expanding the sum for small values of $\Delta\mu^j / \nu R^j T$, we have

$$\sum_j c_\Gamma^j \left(\frac{\Delta\mu^j}{T} - \frac{(\Delta\mu^j)^2}{\nu R^j T^2} + \cdots\right) = 0 \tag{172}$$

and thus

$$\sigma = \Gamma \sum_j c_\Gamma^j \frac{\Delta\mu^j}{T} \approx \Gamma \sum_j \frac{c_\Gamma^j (\Delta\mu^j)^2}{\nu R^j T^2}$$

$$\approx \Gamma \sum_j \nu R^j c_\Gamma^j \left(\frac{Q_x}{K_x} - 1\right)^2 > 0. \tag{173}$$

Since the two phases are not in chemical equilibrium for fractional melting, there is a chemical potential difference between the two phases and thus a positive entropy production according to the above expression. However, in practice this entropy production is very slight and the sum in the above is usually much less than the latent heat.

It should also be noted that in the case of a single component, incrementally isentropic fractional fusion differs from equilibrium melting, but thermally equilibrated fractional melting is identical to equilibrium melting. For a single component, if the two phases have the same thermodynamic pressure and the same temperature then they must be in thermodynamic equilibrium with one another. For two or more components the two phases can differ in chemical composition whilst having the same temperature and pressure and thus are not necessarily in equilibrium.

As the Damköhler numbers are reduced, the kinetics of melting becomes slower and the reactive boundary layers, which occur on the onset of melting, grow. An example of these boundary layers can be seen in Fig. 3 (solid lines). The structure of these boundary layers is fairly intuitive: The temperature gradient initially follows the solid adiabatic gradient and there is initially no melting. As the degree of disequilibrium grows and the kinetics get faster the temperature gradient transitions to that of equilibrium melting and the productivity transitions to the equilibrium melt productivity.

For the single component case, the reactive boundary layers can be treated analytically and this is done in Section D. The boundary layer thickness for a single component is given by

$$l_\Gamma = \frac{\rho_s v_0 C_s T_0^2}{\lambda_\Gamma L^2} = \frac{\nu R C_s T_0^2 \Delta z}{L^2 \mathrm{Da}_\Gamma}, \qquad (174)$$

where T_0 is the temperature at the onset of melting. The non-dimensional quantity $\nu R C_s T_0^2/L^2$ is similar for both pure forsterite (0.95) and pure fayalite (0.87) (Table 1) and is close to 1. Thus for the binary case, an approximate boundary layer thickness of $l_\Gamma \approx \Delta z/\mathrm{Da}_\Gamma$ is expected and indeed this is what is seen in Fig. 3 where $\mathrm{Da}_\Gamma = 10$: The pressure drop across the boundary layer is on the order of 1 GPa, which is a tenth of the total pressure drop over the column. It should be noted that the value of $\mathrm{Da}_\Gamma = 10$ in Fig. 3 is chosen simply to demonstrate the boundary layer structure; realistic Damköhler numbers are likely to be much larger.

10.3 Full numerical solution

Fig. 4 shows a full numerical solution of a 1-D column without the approximations of the previous section. To avoid the singularities at the onset of melting associated with zero porosities, initial conditions are chosen with a small initial degree of melting $F_0 = 5 \times 10^{-5}$ with initial porosity ϕ_0 and initial upwelling rate v_0 such that there is initially no separation of melt from residue that is, zero initial Darcy flux $q_0 = 0$. This is somewhat unphysical (Sramek *et al.* 2007), but is a simple way to remove the initial singularity. The zero compaction length solution is also shown on the figure (dotted line) and was used as an initial guess for the full numerical solver, which is a standard two point boundary value problem solver.

Similar to Fig. 3, Fig. 4 shows near-equilibrium ($\mathrm{Da}_\Gamma = 50$, $\mathrm{Da}_J = 50$) and near-fractional ($\mathrm{Da}_\Gamma = 50$, $\mathrm{Da}_J = 0$) scenarios. As in the earlier calculations, the differences between the two cases is slight. The most notable difference is in the fluid composition c_f, as would be expected. Also as expected, the zero compaction length approximation is a good approximation for most of the melting column, with the exception of the bottom boundary. At the top of the melting column, the zero compaction length solution is exact, as a result of the free flux boundary condition applied there.

There is a reactive boundary layer at the onset of melting and this is visible in Fig. 4 in the build up of compaction pressure at the base of the column. From the Damköhler number, the expected reactive boundary layer thickness is around 1.2 km. The structure of the boundary layer can be seen more clearly in Fig. 5 which shows a zoomed in view of the first 5 km of the column. The zero compaction length approximation provides a reasonable estimate of the structure of the reactive boundary layer, but there are differences. The most notable difference is in the first 0.5 km, where there is a further inner boundary layer. The structure of this inner boundary layer is a result of the finite porosity, zero Darcy flux initial conditions used to avoid the initial singularity and is unphysical. Further asymptotic
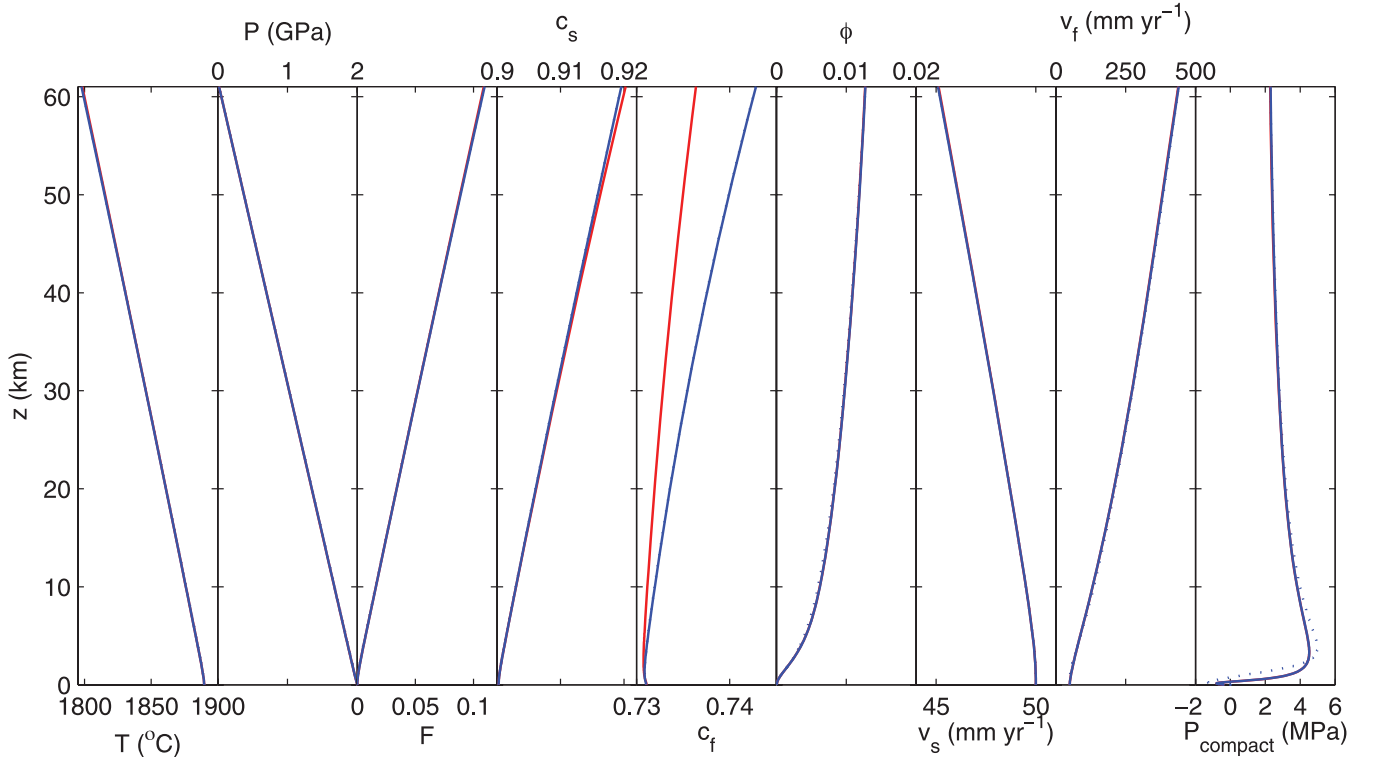

Figure 4. 1-D binary melting column calculations. Blue line is near-equilibrium ($\mathrm{Da}_\Gamma = 50$, $\mathrm{Da}_J = 50$) and red line is near-fractional ($\mathrm{Da}_\Gamma = 50$, $\mathrm{Da}_J = 0$). Dotted line shows the zero compaction length approximation for the near equilibrium case. From left to right: temperature T, fluid pressure P, degree of melting F, solid composition c_s, fluid composition c_f, porosity ϕ, solid velocity V, fluid velocity v, compaction pressure $\tilde{P}$. The difference between near-equilibrium and near-fractional is most notable in the fluid composition c_f, whereas in the other variables there is little difference.
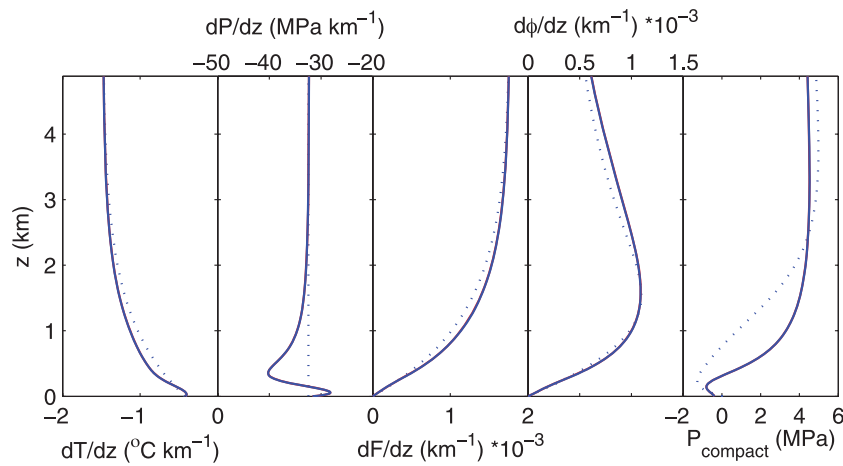
Figure 5. A zoomed-in view of the reactive boundary layer of Fig. 4. The boundary layer structure is clearest in the derivatives: dT/dz, dP/dz, dF/dz and $d\phi/dz$ are shown here, along with the compaction pressure $\tilde{P}$.

analysis is needed to explore the singularity at the onset of melting for finite kinetic rate, as was done for infinite kinetic rate by Sramek *et al.* (2007) and Hewitt & Fowler (2008), but we do not attempt this here.

The boundary layer structure for dT/dz and dF/dz is largely similar to that of dT/dP and dF/dP in Fig. 3: the temperature gradient transitions from the solid adiabat value to equilibrium melting value and the melting rate starts off at zero and increases to the equilibrium melt productivity. The porosity gradient $d\phi/dz$ initially increases in a similar manner to dF/dz, but then decreases: Initially, there is no separation of melt from matrix, but as the porosity increases, permeability increases. Melt then separates from the matrix and porosity increases at a lower rate. A similar effect occurs in the compaction pressure profile: $\tilde{P}$ changes sign as we go from a situation where melt is initially locked to the matrix (so the matrix must dilate as a result of melting, $\tilde{P} < 0$) to one where melt can flow freely and the matrix can compact ($\tilde{P} > 0$). The compaction pressure is directly related to the rate of melting and the build up in compaction pressure reflects the increase in the rate of melting.

It should be reiterated that the Damköhler numbers used in the above calculations are demonstrative rather than necessarily realistic. The reactive length scale for mantle melting is around 10 m (Aharonov *et al.* 1995) and so in practice the reactive boundary layers at the onset of melting are negligible in extent. Nevertheless, reactive boundary layers are an important feature of the disequilibrium equations.

11 CONCLUSIONS

The main outcome of this work is a framework for studying disequilibrium two phase multicomponent flow that generalises the familiar batch and fractional models of melting. Two simple melting problems have been addressed which give a flavour of the behaviour of the equations, but the more interesting problems that need to be tackled next are time-dependent, two or three dimensional, with two or more components and require a more detailed numerical study. Existing geodynamic codes already model equilibrium two phase multicomponent flow (e.g. Katz 2008) and hopefully only small modifications of these codes will be needed to address disequilibrium.

Perhaps the most important problem to revisit is the reaction infiltration instability (Aharonov *et al.* 1995; Spiegelman *et al.* 2001).

This channelling instability relies on having at least two components and two dimensions. Current models of the instability have used somewhat ad hoc laws for interphase mass transfer: With the framework presented here connections could be made to real phase diagrams, and melting can occur in a self-consistent energy conserving manner rather than as an ad hoc imposed function of depth. Some further analytical work on reaction infiltration may be possible, such as a linear stability analysis of the two component equations, but most future work will need detailed numerics.

REFERENCES

Agee, C.B., 1992. Thermal expansion of molten Fe_2SiO_4 at high pressure, *Geophys. Res. Lett.,* **19,** 1173–1176.

Aharonov, E., Whitehead, J.A., Kelemen, P.B. & Spiegelman, M., 1995. Channeling instability of upwelling melt in the mantle, *J. geophys. Res.,* **100,** 20 433–20 450.

Ahern, J.L. & Turcotte, D.L., 1979. Magma migration beneath an ocean ridge, *Earth planet. Sci. Lett,* **45,** 115–122.

Ahrens, T.J., (ed.) 1995. *Mineral Physics and Crystallography : a Handbook of Physical Constants,* AGU, Washington, D.C., ISBN 0-87590-852-7.

Anderson, G.M., 2005. *Thermodynamics of Natural Systems,* Cambridge University Press, Cambridge.

Asimow, P.D., 2002. Steady state mantle-melt interaction in one dimension: II. Thermal interactions and irreversible terms, *J. Petrol.,* **43,** 1707–1724.

Asimow, P.D. & Stolper, E.M., 1999. Steady-state mantle-melt interactions in one dimension: I. Equilibrium transport and melt focusing, *J. Petrol.,* **40,** 475–494.

Asimow, P.D., Hirschmann, M.M. & Stolper, E.M., 1997. An analysis of variations in isentropic melt productivity, *Phil. Trans. R. Soc. Lond. A,* **355,** 255–281.

Baker, J. & Cahn, J.W., 1971. *Solidification,* p. 23, Am. Soc. Metals, Metals Park, Ohio.

Bercovici, D. & Ricard, Y., 2003. Energetics of a two-phase model of lithospheric damage, shear localization and plate-boundary formation, *Geophys. J. Int.,* **152,** 581–596.

Bercovici, D., Ricard, Y. & Schubert, G., 2001. A two-phase model for compaction and damage 1. General theory, *J. geophys. Res.,* **106,** 8887–8906.

Bottinga, Y., 1985. On the thermal compressibility of silicate liquids at high pressure, *Earth planet. Sci. Lett,* **74,** 350–360.

Bradley, R.S., 1962. Thermodynamic calculations on phase equilibra involving fused salts, part II, Solid solutions and applications to olivines, *Am. J. Sci.,* **260,** 550–554.

Caroli, B., Caroli, C. & Roulet, B., 1986. Interface kinetics and solidification of alloys: a discussion of some phenomenological models, *Acta Metall.,* **34,** 1867–1877.

Chakraborty, S., 1997. Rates and mechanisms of Fe-Mg interdiffusion in olivine at $980° − 1300°C$, *J. geophys. Res.,* **102,** 12 317–12 331.

Connolly, J.A.D. & Podladchikov, Y.Y., 1998. Compaction-driven fluid flow in viscoelastic rock, *Geodinamica Acta,* **11,** 55–84.

de Groot, S.R. & Mazur, P., 1984. *Non-equilibrium Themodynamics,* Dover, Mineola, NY, ISBN 978-0486647418.

Deer, W.A., Howie, R.A. & Zussman, J., 1992. *An Introduction to the Rock-forming Minerals - 2nd edition,* Prentice Hall, Harlow.

Drew, D.A., 1983. Mathematical modeling of two-phase flow, *Ann. Rev. Fluid Mech.,* **15,** 261–291.

Fowler, A.C., 1985. A mathematical model of magma transport in the asthenosphere, *Geophys. Astophys. Fluid Dyn.,* **33,** 63–96.

Hewitt, I.J. & Fowler, A.C., 2008. Partial melting in an upwelling mantle column, *Proc. Roy. Soc. A,* **464,** 2467–2491.

Hillert, M., 2006. An application of irreversible thermodynamics to diffusional phase transformations, *Acta Mater.,* **54,** 99–104.

Katz, R.F., 2008. Magma dynamics with the enthalpy method: benchmark solutions and magmatic focusing at mid-ocean ridges, *J. Petrol.,* **49,** 2099–2121.

Kelemen, P.B., Hirth, G., Shimizu, N., Spiegelman, M. & Dick, H.J.B., 1997. A review of melt migration processes in the adiabatically upwelling mantle beneath oceanic spreading ridges, *Phil. Trans. R. Soc. Lond. A,* **355,** 283–318.

Lasaga, A.C., 1998. *Kinetic Theory in the Earth Sciences,* Princeton University Press, Princeton, NJ.

Liang, Y., 2003. Kinetics of crystal-melt reaction in partially molten silicates: 1. Grain scale processes, *Geochem. Geophys. Geosyst.,* **4,** 1045, doi:10.1029/2002GC000375.

Maaløe, S., 1984. Fractional crystallization and melting within binary system with solid solution, *Am. J. Sci.,* **284,** 272–287.

McKenzie, D., 1984. The generation and compaction of partially molten rock, *J. Petrol.,* **25,** 713–765.

Poirier, J.-P., 2000. *Introduction to the Physics of the Earth's Interior,* Cambridge University Press, Cambridge.

Ribe, N.M., 1985a. The generation and composition of partial melts in the earth's mantle, *Earth planet. Sci. Lett.,* **73,** 361–376.

Ribe, N.M., 1985b. The deformation and compaction of partial molten zones, *Geophys. J. R. astr. Soc.,* **83,** 487–501.

Ricard, Y., 2007. Physics of mantle convection, in *Treatise on Geophysics,* chapter 7.02, pp. 31–87, ed. Schubert, G., Elsevier, Amsterdam.

Ricard, Y., Bercovici, D. & Schubert, G., 2001. A two-phase model for compaction and damage 2. Applications to compaction, deformation, and the role of interfacial surface tension, *J. geophys. Res.,* **106,** 8907–8924.

Schmeling, H., 2000. Partial melting and melt segregation in a convecting mantle, in *Physics and Chemistry of Partially Molten Rocks,* pp. 141–178, eds Bagdassarov, N., Laporte, D. & Thompson, A.B., Kluwer, Dordrecht.

Scott, D.R. & Stevenson, D.J., 1984. Magma solitons, *Geophys. Res. Lett.,* **11,** 1161–1164.

Simpson, G., Spiegelman, M. & Weinstein, M.I., 2010a. A multiscale model of partial melts:1. Effective equations, *J. geophys. Res.,* **115,** B04410, doi:10.1029/2009JB006375.

Simpson, G., Spiegelman, M. & Weinstein, M.I., 2010b. A multiscale model of partial melts: 2. Numerical results, *J. geophys. Res.,* **115,** B04411, doi:10.1029/2009JB006376.

Spear, F.S., 1993. *Metamorphic Phase Equilibria and Pressure-Temperature-Time Paths,* Mineralogical Society of America, Washington, D.C., ISBN 0939950340.

Spera, F.J. & Trial, A.F., 1993. Verification of the Onsager reciprocal relations in a molten silicate solution, *Science,* **259,** 204–206.

Spiegelman, M., 1993a. Flow in deformable porous media. Part 1 Simple analysis, *J. Fluid Mech.,* **247,** 17–38.

Spiegelman, M., 1993b. Flow in deformable porous media. Part 2 Numerical analysis - the relationship between shock waves and solitary waves, *J. Fluid Mech.,* **247,** 39–63.

Spiegelman, M., 1996. Geochemical consequences of melt transport in 2-D: the sensitivity of trace elements to mantle dynamics, *Earth planet. Sci. Lett,* **139,** 115–132.

Spiegelman, M. & Elliott, T., 1993. Consequences of melt transport for U-series disequilibrium in young lavas, *Earth planet. Sci. Lett,* **118,** 1–20.

Spiegelman, M., Kelemen, P.B. & Aharonov, E., 2001. Causes and consequences of flow organization during melt transport: the reaction infiltration instability in compactible media, *J. geophys. Res.,* **106,** 2061–2077.

Sramek, O., Ricard, Y. & Bercovici, D., 2007. Simultaneous melting and compaction in deformable two-phase media, *Geophys. J. Int.,* **168,** 964–982.

Stolper, E. & Asimow, P., 2007. Insights into mantle melting from graphical analysis of one-component systems, *Am. J. Sci.,* **307,** 1051–1139.

Tackley, P.J. & Stevenson, D.J., 1993. A mechanism for spontaneous self-perpetuating volcanism on the terrestrial planets, in *Flow and Creep in the Solar System: Observations, Modeling and Theory,* pp. 307–321, eds Stone, D.B. & Runcorn, S.K., Kluwer, Dordrecht.

Tirone, M., Ganguly, J. & Morgan, J.P., 2009. Modeling petrological geodynamics in the earth's mantle, *Geochem. Geophys. Geosyst.,* **10,** Q04012, doi:10.1029/2008GC002168.

APPENDIX A: THE RELATIONSHIPS BETWEEN PRESSURES

A detailed description of the relationships between interface pressure, fluid pressure and solid pressure was given by Bercovici & Ricard (2003) and Ricard (2007), and is reiterated in outline below. Bercovici & Ricard (2003) assumed the interface pressure to be a linear combination of the fluid and solid pressures,

$$P = (1 − ω)p_f + ωp_s, \tag{A1}$$

where $ω$ quantifies the partitioning of surface energy. $ω = 0$ corresponds to the case described by McKenzie (1984). In terms of pressure differences, (A1) can be written as

$$P − p_f = ω\Delta p, \tag{A2}$$

$$P − p_s = −(1 − ω)\Delta p, \tag{A3}$$

where $\Delta p \equiv p_s − p_f$ is the mechanical pressure difference between solid and fluid. The viscous dissipation (33) then becomes

$$\Psi = d\left(\mathbf{v}_f − \mathbf{v}_s\right)^2 + \Delta p\left(\phi ω \nabla \cdot \mathbf{v}_f − (1 − \phi)(1 − ω)\nabla \cdot \mathbf{v}_s\right) + \phi\boldsymbol{\tau}_f : \nabla \mathbf{v}_f + (1 − \phi)\boldsymbol{\tau}_s : \nabla \mathbf{v}_s. \tag{A4}$$

The above form of the viscous dissipation suggests a linear phenomenological law of the form

$$\Delta p = B\left(\phi ω \nabla \cdot \mathbf{v}_f − (1 − \phi)(1 − ω)\nabla \cdot \mathbf{v}_s\right), \tag{A5}$$

provided there is no coupling with the other scalar thermodynamic fluxes (Sramek *et al.* 2007). The form of the phenomenological coefficient B is unknown and will depend on parameters such as porosity. If we write the coefficient $B = \zeta_\phi/(1 − ω − \phi)^2$ such that the phenomenological law is written as

$$\Delta p = \zeta_\phi \frac{\left(\phi ω \nabla \cdot \mathbf{v}_f − (1 − \phi)(1 − ω)\nabla \cdot \mathbf{v}_s\right)}{(1 − ω − \phi)^2}, \tag{A6}$$

then ζ_ϕ can be identified with the effective bulk viscosity used by McKenzie (1984). When $ω = 0$, eqs (A2) and (A3) with (A6) are identical to (25) and (26). The advantage of (A2), (A3) and (A6) is

that they are clearly symmetric: they are invariant under the change $\phi \leftrightarrow 1-\phi$, $\omega \leftrightarrow 1-\omega$, $p_f \leftrightarrow p_s$, $\mathbf{v}_f \leftrightarrow \mathbf{v}_s$ (assuming the effective bulk viscosity ζ_ϕ obeys this same symmetry).

In Bercovici *et al.* (2001) the symmetric form

$$B = \frac{K_0 \left(\mu_f + \mu_s\right)}{\phi(1 - \phi)} \tag{A7}$$

is suggested for the phenomenological coefficient B, where K_0 is a constant, and μ_f and μ_s are the true (rather than effective) viscosities of fluid and solid. The corresponding deviatoric stress tensors are given by

$$\boldsymbol{\tau}_f = \mu_f \left(\nabla \mathbf{v}_f + \nabla \mathbf{v}_f^T - \frac{2}{3} \left(\nabla \cdot \mathbf{v}_f\right) \mathbf{I}\right), \tag{A8}$$

$$\boldsymbol{\tau}_s = \mu_s \left(\nabla \mathbf{v}_s + \nabla \mathbf{v}_s^T - \frac{2}{3} \left(\nabla \cdot \mathbf{v}_s\right) \mathbf{I}\right). \tag{A9}$$

When the fluid is much less viscous than the solid, $\mu_f \ll \mu_s$, these reduce to (27) and (28), provided $\eta_\phi \to \mu_s(1 - \phi)$ in this limit.

Another way of writing the phenomenological laws is in terms of an effective pressure p_e, which can be defined as the difference between mean mechanical pressure $\overline{p}$ and interface pressure P (*cf.* Connolly & Podladchikov 1998). The effective pressure p_e is linearly related to the pressure difference Δp by

$$p_e \equiv \overline{p} - P = (1 - \omega - \phi)\Delta p. \tag{A10}$$

Thus a phenomenological law for effective pressure is

$$p_e = \zeta_\phi \frac{\left(\phi\omega\nabla \cdot \mathbf{v}_f - (1 - \phi)(1 - \omega)\nabla \cdot \mathbf{v}_s\right)}{(1 - \omega - \phi)}. \tag{A11}$$

When $\omega = 0$, $p_e = -\zeta_\phi\nabla \cdot \mathbf{v}_s$ and when $\omega = 1$, $p_e = -\zeta_\phi\nabla \cdot \mathbf{v}_f$. Further discussion of the pressure relationships can be found in Simpson *et al.* (2010a).

APPENDIX B: VECTOR PHENOMENOLOGICAL LAWS

The derivation of intraphase phenomenological laws for fluxes of heat and mass follows directly from the derivation for single phase fluids which is described in detail by de Groot & Mazur (1984) and a brief summary is given here. It is useful to use the alternative definition of heat flux given in (52). The entropy flux (41) can then be written as

$$\mathbf{j} = \frac{\mathbf{q}'}{T} + \sum_j \mathbf{J}_f^j s_f^j + \mathbf{J}_s^j s_s^j, \tag{B1}$$

where s_f^j and $ß^j$ are the specific entropies per components. The corresponding entropy production (42) can be written as

$$T\sigma = Q + \Psi - \frac{\mathbf{q}'}{T} \cdot \nabla T + \sum_j \Gamma^j \Delta\mu^j - \mathbf{J}_f^j \cdot \nabla_T\mu_f^j - \mathbf{J}_s^j \cdot \nabla_T\mu_s^j \tag{B2}$$

since

$$T\nabla\left(\frac{\mu_f^j}{T}\right) = \nabla_T\mu_f^j - \frac{h_f^j}{T}\nabla T = \nabla\mu_f^j - \frac{\mu_f^j}{T}\nabla T \tag{B3}$$

and $\mu_f^j = h_f^j - Ts_f^j$. ∇_T refers to gradients at fixed temperature.

The entropy production due to vector fluxes is given from (B2) as

$$\sigma = -\frac{\mathbf{q}'}{T^2} \cdot \nabla T - \sum_j \mathbf{J}_f^j \cdot \frac{\nabla_T\mu_f^j}{T} - \sum_j \mathbf{J}_s^j \cdot \frac{\nabla_T\mu_s^j}{T}. \tag{B4}$$

This suggests linear phenomenological laws of the form

$$\mathbf{q}' = -A\frac{\nabla T}{T^2} - \sum_k \frac{B_f^k \nabla_T\mu_f^k}{T} - \sum_k \frac{B_s^k \nabla_T\mu_s^k}{T}, \tag{B5}$$

$$\mathbf{J}_f^j = -C_f^j\frac{\nabla T}{T^2} - \sum_k \frac{L_{ff}^{jk}\nabla_T\mu_f^k}{T} - \sum_k \frac{L_{fs}^{jk}\nabla_T\mu_s^k}{T}, \tag{B6}$$

$$\mathbf{J}_s^j = -C_s^j\frac{\nabla T}{T^2} - \sum_k \frac{L_{sf}^{jk}\nabla_T\mu_f^k}{T} - \sum_k \frac{L_{ss}^{jk}\nabla_T\mu_s^k}{T}. \tag{B7}$$

However, the forces and fluxes here are not independent, as there are linear relations between them. The diffusive mass fluxes of components are constrained by conservation of mass through (12)

$$\sum_j \mathbf{J}_f^j = \sum_j \mathbf{J}_s^j = 0, \tag{B8}$$

and the forces are constrained by Gibbs–Duhem equations for the two phases,

$$\sum_j c_f^j\nabla\mu_f^j = -s_f\nabla T + \frac{1}{\rho_f}\nabla P, \tag{B9}$$

$$\sum_j c_s^j\nabla\mu_s^j = -s_s\nabla T + \frac{1}{\rho_s}\nabla P, \tag{B10}$$

which can be rewritten using (B3) as

$$\sum_j \rho_f c_f^j\nabla_T\mu_f^j = \nabla P, \tag{B11}$$

$$\sum_j \rho_s c_s^j\nabla_T\mu_s^j = \nabla P. \tag{B12}$$

The right hand side in the above is often neglected (see de Groot & Mazur 1984, Chapter 11), but this assumes mechanical equilibrium.

When there exist linear relationships between the forces and fluxes there are two ways to proceed. Either one can use the linear relationships to define a new set of independent fluxes and forces, or one can keep the existing fluxes and forces and acknowledge that there are constraints on the coefficients. Without independent fluxes and forces, the phenomenological coefficients are not unique, however they can always be chosen such that the Onsager reciprocal relations hold (see de Groot & Mazur 1984, chapter 6). In this case, the Onsager reciprocal relations are

$$B_f^j = C_f^j, \quad B_s^j = C_s^j, \tag{B13}$$

$$L_{ff}^{jk} = L_{ff}^{kj}, \quad L_{fs}^{jk} = L_{sf}^{kj}, \quad L_{ss}^{jk} = L_{ss}^{kj}. \tag{B14}$$

For the sake of simplicity, it is helpful to assume that a lot of these cross couplings are negligible and reduce the above to simplified phenomenological laws, for example,

$$\mathbf{q}' = -k_T\nabla T \tag{B15}$$

$$\mathbf{J}_f^j = -\phi\rho_f \sum_{k=1}^{n-1} D_f^{jk}\nabla c_f^k, \quad j = 1, 2, \ldots, n - 1 \tag{B16}$$

$$\mathbf{J}_s^j = -(1 - \phi)\rho_s \sum_{k=1}^{n-1} D_s^{jk}\nabla c_s^k, \quad j = 1, 2, \ldots, n - 1 \tag{B17}$$

$$\mathbf{J}_f^n = -\sum_{k=1}^{n-1} \mathbf{J}_f^j \tag{B18}$$

$$\mathbf{J}_s^n = -\sum_{k=1}^{n-1} \mathbf{J}_s^j, \tag{B19}$$

where k_T is the effective thermal conductivity of the mixture and D_f^{jk} and D_s^{jk} are intra-phase effective diffusion coefficients for the melt and the matrix. Eq. (B15) is Fourier's law of heat flow and (B16) and (B17) are the appropriate generalisations of Fick's law of diffusion. The word 'effective' should be emphasised here—the diffusion coefficients are not necessarily the same as for a single phase fluid and can be controlled by phenomena such Taylor dispersion. Moreover, the diffusion might not be isotropic as is assumed in the laws above and a more general treatment would have second rank diffusivity tensors. It should also be noted that due to Onsager's reciprocal relations, there are only $n(n-1)/2$ independent coefficients in each of D_f^{jk} and D_s^{jk}. In particular, note that it is not possible to choose D_f^{jk} and D_s^{jk} as diagonal matrices, unless the diffusivities are all the same. For a more detailed exposition of the constraints on diffusion coefficients and the coupling between heat flow and mass transport (the Soret and Dufour effects), the reader is encouraged to consult the textbooks (see Lasaga 1998; de Groot & Mazur 1984). Onsager's reciprocal relationships were verified experimentally for molten silicates by Spera & Trial (1993).

APPENDIX C: CRYSTALLISATION

Although our main focus in this work is on generalisations of fractional melting, it should be noted that fractional crystallisation can be described in a similar way. The phenomenological laws (82)–(83) have to be adjusted slightly to read

$$\Gamma^j = \sum_k E^{jk} Z^k, \tag{C1}$$

$$Z^k = \nu R^k \left(\left(\frac{Q^k}{K^k} \right)^{1/\nu} - 1 \right) = \nu R^k \left(\frac{x_s^k}{K_x^k x_f^k} - 1 \right). \tag{C2}$$

Type I crystallising has $x_\Gamma^j = x_f^j$ and type II crystallising has $x_\Gamma^j = \left\{ K_x^j x_s^j \right\}$. It should be noted that related phenomenological laws for interphase mass transfer were proposed by Liang (2003) based on averaging a grain scale model. Two regimes were identified, and the terminology used here is based on Liang (2003). Regime I of Liang (2003) (diffusion-in-melt-limited dissolution) is essentially type I melting and regime II (diffusion-in-solid-limited precipitation) is essentially type II crystallising.

APPENDIX D: SINGLE COMPONENT MELTING

A number of simple analytical expressions exist for the single component 1-D melting column. In this section, we will make the zero compaction length approximation, assume pressure can be treated as approximately lithostatic ($dP/dz = -\rho_s g$) and assume constant densities except for the adiabatic gradient term. The phenomenological law for melting is

$$\Gamma = \lambda_\Gamma \nu R \left(1 - \exp \left(\frac{L}{\nu R} \left(\frac{1}{T} - \frac{1}{T_m(P)} \right) \right) \right). \tag{D1}$$

For small deviations in temperature from equilibrium (i.e. rapid kinetics), the above law can be linearised as

$$\Gamma = \frac{\lambda_\Gamma L}{T_0^2} (T - T_m(P)), \tag{D2}$$

where T_0 is the temperature at the onset of melting. A natural scale for temperature differences during melting is L/C and we may write

$$T = T_0 + \frac{L}{C} \Theta, \tag{D3}$$

$$T_m = T_0 + \left. \frac{dT_m}{dP} \right|_{T_0} (P - P_0) = T_0 - \rho_s g \left. \frac{dT_m}{dP} \right|_{T_0} z = T_0 - \frac{L}{C} \frac{z}{l_m}, \tag{D4}$$

assuming an approximately linear Clapeyron slope. l_m is a natural length scale for temperature changes during melting, given by

$$l_m = \frac{L}{\rho_s g C \, dT_m/dP|_{T_0}}. \tag{D5}$$

The phenomenological law for melting can then be written as

$$\Gamma = \frac{\lambda_\Gamma L^2}{C T_0^2} \left(\Theta + \frac{z}{l_m} \right) = \frac{\rho_s v_0}{l_\Gamma} \left(\Theta + \frac{z}{l_m} \right) \tag{D6}$$

where l_Γ is a reactive length scale,

$$l_\Gamma = \frac{\rho_s v_0 C T_0^2}{\lambda_\Gamma L^2}. \tag{D7}$$

The ratio of the two length scales l_m and l_Γ defines a Damköhler number,

$$\mathrm{Da}_\Gamma^* = \frac{l_m}{l_\Gamma} = \frac{\lambda_\Gamma L^3}{\rho_s^2 v_0 C^2 T_0^2 \, dT_m/dP|_{T_0}}. \tag{D8}$$

Note that this differs from the Damköhler numbers defined in the main text which are based on scaling by the column height.

The steady state 1-D column equations can be nondimensionalised using $z = z' l_m$, $\Gamma = \Gamma' \rho_s v_0 / l_m$. The non-dimensional governing equations are, using (132), (137) and (D6),

$$\frac{dF}{dz} = \Gamma, \tag{D9}$$

$$\frac{d\Theta}{dz} = -\mathcal{A}^* (1 + \mathrm{St}^* \Theta) - \Gamma, \tag{D10}$$

$$\Gamma = \mathrm{Da}_\Gamma^* (\Theta + z), \tag{D11}$$

where

$$\mathcal{A}^* = \frac{\alpha_s T_0}{\rho_s C \, dT_m/dP|_{T_0}}, \qquad \mathrm{St}^* = \frac{L}{C T_0}. \tag{D12}$$

$\mathcal{A}^*$ is the adiabatic parameter and St^* is a Stefan number. At the onset of melting $F = 0$ and $\Theta = 0$. The boundary layer structure is apparent when the equations are rescaled using $\epsilon = (\mathrm{Da}_\Gamma^*)^{-1}$ (a small parameter for rapid kinetics) with $z = \epsilon y$, $F = \epsilon f$, $\Theta = \epsilon \theta$. To leading order in ϵ,

$$\frac{df}{dy} = \Gamma, \tag{D13}$$

$$\frac{d\theta}{dy} = -\mathcal{A}^* - \Gamma, \tag{D14}$$

$$\Gamma = \theta + y, \tag{D15}$$

with $f(0) = 0$ and $\theta(0) = 0$. These integrate to give

$$\theta(y) = -y + (1 - \mathcal{A}^*)(1 - e^{-y}), \tag{D16}$$

$$f(y) = (1 - \mathcal{A}^*)\left(y - 1 + e^{-y}\right), \tag{D17}$$

with derivatives

$$\frac{d\theta}{dy} = -1 - (1 - \mathcal{A}^*)(1 - e^{-y}), \tag{D18}$$

$$\frac{df}{dy} = (1 - \mathcal{A}^*)\left(1 - e^{-y}\right). \tag{D19}$$

In dimensional form, the above can be written as

$$\frac{dT}{dz} = -\frac{\alpha_s g T_0}{C} - \left(\rho_s g \left.\frac{dT_m}{dP}\right|_{T_0} - \frac{\alpha_s g T_0}{C}\right)\left(1 - e^{-z/l_\Gamma}\right), \tag{D20}$$

$$\frac{dF}{dz} = \frac{C}{L}\left(\rho_s g \left.\frac{dT_m}{dP}\right|_{T_0} - \frac{\alpha_s g T_0}{C}\right)\left(1 - e^{-z/l_\Gamma}\right), \tag{D21}$$

eqs (D20) and (D21) are fairly intuitive: The gradient in temperature starts off at the solid adiabatic gradient and ends up at the Clapeyron slope and the melt productivity starts off at zero and ends up at the same productivity as for equilibrium batch melting (Asimow *et al.* 1997). The boundary layer thickness is controlled by the reactive length l_Γ which shrinks as the reaction rate increases or the upwelling rate slows.

The dimensional temperature and degree of melting profiles are

$$T = T_0 - \rho_s g \left.\frac{dT_m}{dP}\right|_{T_0} z + \left(\rho_s g \left.\frac{dT_m}{dP}\right|_{T_0} - \frac{\alpha_s g T_0}{C}\right) l_\Gamma \left(1 - e^{-z/l_\Gamma}\right), \tag{D22}$$

$$F = \frac{C}{L}\left(\rho_s g \left.\frac{dT_m}{dP}\right|_{T_0} - \frac{\alpha_s g T_0}{C}\right)\left(z - l_\Gamma \left(1 - e^{-z/l_\Gamma}\right)\right). \tag{D23}$$

Outside the boundary layer ($z \gg l_\Gamma$), these can be written as

$$T = T_m(z) + \frac{L}{C} \left.\frac{dF_m}{dz}\right|_{T_0} l_\Gamma, \tag{D24}$$

$$F = F_m(z) - \left.\frac{dF_m}{dz}\right|_{T_0} l_\Gamma, \tag{D25}$$

where F_m is defined to be the degree of melting for equilibrium melting ($Da_\Gamma^* \to \infty$). Thus there is small degree of superheating ($T > T_m$) and a slightly lower degree of melting ($F < F_m$) that exists throughout the column as a result of the finite kinetics.

The boundary layer structure outlined above is very similar to that found in the reaction infiltration instability problem described by Aharonov *et al.* (1995). However, there is an important difference between the Aharonov *et al.* (1995) problem and the single component melting described above: For reaction infiltration, differences in concentration cause interphase mass transfer, whereas here interphase mass transfer is caused by differences in temperature. Concentration perturbations are advected with the fluid velocity in the Aharonov *et al.* (1995) problem, whereas temperature perturbations here travel more slowly, at the mean upwelling velocity ($\overline{v}$). As a result, the single component melting equations are stable and do not have a reaction infiltration instability.

The stability can be demonstrated as follows. In 1-D, total conservation of mass is

$$\frac{\partial \overline{\rho}}{\partial t} + \frac{\partial}{\partial z}\left(\overline{\rho v}\right) = 0. \tag{D26}$$

Porosities are typically small ($\phi \ll 1$) and thus $\overline{\rho} \approx \rho_s$ and $\overline{\rho v} \approx \rho_s v_0$. Neglecting the adiabat, conservation of energy is then

$$\rho_s C \frac{\partial T}{\partial t} + \rho_s v_0 C \frac{\partial T}{\partial z} = -\Gamma L, \tag{D27}$$

which in non-dimensional variables is

$$\frac{\partial \Theta}{\partial t} + \frac{\partial \Theta}{\partial z} = -Da_\Gamma \left(\Theta + z\right). \tag{D28}$$

Where an appropriate time scale for non-dimensionalising is $t_0 = l_m/v_0$. Solutions to this equation can be sought in terms of perturbations about the steady state, $\Theta = \overline{\Theta}(z) + \varepsilon e^{imz+\sigma t}$. Neglecting boundary layers, a suitable steady state is

$$\overline{\Theta}(z) = -z + \frac{1}{Da_\Gamma}, \tag{D29}$$

and the growth rate of perturbations is

$$\sigma = -Da_\Gamma - im. \tag{D30}$$

Hence any perturbations in temperature will simply decay away.